



RESEARCH MEMORANDUM

EFFECTS OF SOME EXTERNAL-STORE MOUNTING ARRANGEMENTS AND
STORE SHAPES ON THE BUFFET AND DRAG CHARACTERISTICS
OF WINGLESS ROCKET-POWERED MODELS AT

MACH NUMBERS FROM 0.7 TO 1.4

By Homer P. Mason and Allen B. Henning

Langley Aeronautical Laboratory
Langley Field, Va.

**NATIONAL ADVISORY COMMITTEE
FOR AERONAUTICS
WASHINGTON**

December 6, 1954
Declassified September 17, 1958

NATIONAL ADVISORY COMMITTEE FOR AERONAUTICS

RESEARCH MEMORANDUM

EFFECTS OF SOME EXTERNAL-STORE MOUNTING ARRANGEMENTS AND
STORE SHAPES ON THE BUFFET AND DRAG CHARACTERISTICS
OF WINGLESS ROCKET-POWERED MODELS AT
MACH NUMBERS FROM 0.7 TO 1.4

By Homer P. Mason and Allen B. Henning

SUMMARY

An investigation of the trim, buffet, and drag characteristics of finless external stores mounted on the fuselage of a wingless rocket-powered research model has been conducted over a Mach number range from 0.7 to approximately 1.4. Configurations investigated consisted of a buffet-free parabolic body and cruciform tail used as a basic vehicle for various arrangements of external stores as follows: a semisubmerged large-diameter bomb shape at two fuselage locations and a cavity representing the condition after release of a bomb at the forward location, a large-diameter bomb shape mounted tangent to the fuselage on a 4-percent-thick pylon and on a 10-percent-thick pylon, a Douglas Aircraft Company, Inc., store shape mounted on a 10-percent-thick pylon, and a Wright Air Development Center store shape mounted on a pylon similar to the Douglas 3 hook shackle pylon, 6 percent thick. Drag studies of models of these store shapes alone were conducted in conjunction with this investigation by using the helium-gun technique.

Results of the investigation are presented to show some effects of store mounting arrangement, store shape, and pylon section on the trim, buffet, and drag characteristics of the configuration. Data are presented as trim normal-force and side-force coefficients, incremental accelerations due to buffeting, and drag coefficients plotted against Mach number. No large or abrupt trim changes may be attributed to the external-store configurations investigated. No buffeting was encountered within the test Mach number range on either of the semisubmerged store configurations; however, mild buffeting was encountered on the cavity model used to simulate the condition after bomb release. Buffeting was encountered throughout the test Mach number range on all models having completely external stores. Severe store buffeting was encountered on the configuration having the large-diameter bomb-shape store mounted tangent to

the fuselage. The similar configuration with the store mounted on a 10-percent-thick pylon encountered much less severe store buffeting than did the tangent-mounted store but buffeted more severely than did the similar configuration having a 4-percent-thick pylon. Both the DAS and WADC shapes experienced only mild store buffeting within the test Mach number range. Large installation drag increments were present on all the completely external-store configurations tested and large interference drag increments are indicated. Little or no interference was evident on the semisubmerged stores except at transonic speeds at the forward location. These data indicate that low-lift buffeting and large drag increments can be induced by mutual interference between a fuselage and external-store assembly at both transonic and supersonic speeds, that interference effects on buffeting and drag may be aggravated by fuselage-store proximity, and that pylon effects on drag are generally small as compared with the total installation effects of the test configurations. Of the three store shapes investigated, the DAS shape appears to be most efficient at supersonic speeds.

INTRODUCTION

The use of external fuel tanks and externally mounted bomb loads has given rise to several problems in the operation of high-speed aircraft. Two of the most important of these problems are large increases in drag and a lowering of the airplane buffet boundary, which is in some cases accompanied by an increase in buffet intensity. In most instances, external stores have been located at various positions on the aircraft wings, and a large amount of research has been done to determine the effects of such store installations. A comparatively small amount of research has been conducted to determine the buffet and drag characteristics of fuselage-mounted external stores. Reference 1 presents the results of a rocket-model study of the drag resulting from external stores at various longitudinal positions on a wingless configuration. Reference 2 presents the buffeting and drag characteristics of various arrangements of fuselage-mounted external stores at one longitudinal location on a wingless rocket-powered research model.

The present paper presents results obtained from an extension of the investigation of reference 2. Results are presented from tests of pylon-mounted models of the Douglas Aircraft Company, Inc., store shape and the Wright Air Development Center store shape as well as results from tests of a semisubmerged large-diameter bomb-shape store and the fuselage cavity resulting from its disposal. The trim, buffet, and drag data obtained from these tests are presented herein and compared with similar data reproduced from reference 2.

SYMBOLS

a_n	normal acceleration, g units
a_t	transverse acceleration, g units
A	cross-sectional area of configuration at any station, sq ft
c	pylon chord
C_D	total drag coefficient based on body cross-sectional area, $\frac{\text{Drag}}{qS_f}$
C_{D_S}	drag coefficient of the store alone based on store cross-sectional area, $\frac{\text{Store drag}}{qS_s}$
ΔC_D	installation drag coefficient (store + interference + pylon) based on exposed store cross-sectional area, $\frac{S_f}{S_s} (C_{D_{on}} - C_{D_{off}})$
$C_{N_{trim}}$	trim normal-force coefficient, $\frac{\text{Normal force}}{qS_t}$
$C_{Y_{trim}}$	trim side-force coefficient, $\frac{\text{Side force}}{qS_t}$
Δg	buffet increment
L	fuselage length, ft
M	Mach number
p	local static pressure, lb/sq ft
P_o	free-stream static pressure, lb/sq ft
P	pressure coefficient, $\frac{P - P_o}{q}$
Δp	differential pressure, positive when pressure in cavity is greater than on fuselage surface, lb/sq ft

q	free-stream dynamic pressure, lb/sq ft
R	Reynolds number
S	area, sq ft
V	store volume, cu ft

Subscripts:

f	fuselage
n	nose
s	store
t	tail
on	stores on
off	stores off

MODELS

The dimensions and characteristics of the basic fuselage-tail configuration are shown in figure 1. This is the basic buffet research vehicle of reference 3 with 6-percent-thick tail surfaces. On this basic model were placed finless, externally mounted stores of varying sizes, shapes, and locations (see table I). These mountings are shown in figure 2 and are classified as semisubmerged store mountings in figure 2(a), vertical store locations in figure 2(b), and external-store shapes in figure 2(c). Figure 2 also presents the longitudinal distribution of cross-sectional area for all the models of this investigation. Photographs of all the models are shown as figure 3.

Three different store shapes were employed in this investigation (tables II, III, and IV). They were a large-diameter bomb shape, the DAS shape (ref. 4), and the WADC store shape (similar to the store of ref. 5). Photographs of small models of these store shapes, used in conjunction with this investigation to obtain the drag of the isolated stores, are shown as figure 4.

All pylons used in this investigation had the same plan-form geometry with respect to the stores and were unswept with pylon chord

equal to one-fourth the store length and pylon length equal to one-half the store diameter. Pylon section and dimensions are tabulated in table I with the configuration designations to be used herein.

INSTRUMENTATION

All the models of this investigation had a longitudinal accelerometer located in the nose of the fuselage and a normal and a transverse accelerometer located near the tail root quarter-chord station. The semisubmerged store models (models A and B) also had a normal and a transverse accelerometer located in the nose of the fuselage, and the tangent- and pylon-mounted store models (models D, E, F, G, and H) had a normal and a transverse accelerometer located in the external store. The cavity model (model C) had a normal accelerometer located in the nose. Six pressure cells were also placed in the cavity model. Static-pressure cells were used to measure the absolute static pressure at the maximum diameter of the model 90° from the plane of the fuselage-cavity center line and at a station between the fins directly behind the cavity in the plane of the fuselage-cavity center line. Differential pressure cells were located inside the fuselage to measure, in the plane of maximum cavity depth, the difference in pressure between the cavity indentation and the opposite surface of the fuselage at four longitudinal stations.

All normal and transverse accelerometers had natural frequencies from 75 to 120 cps and 50- to 75-percent critical damping.

TESTS

Shake tests were performed on each model to determine their approximate natural structural frequencies. The approximate natural frequencies and modes of vibration found for the tangent- and pylon-mounted store models are presented in the following table:

Mode	Model D	Model E	Model F	Model G	Model H
Pylon bending, cps	108	82, 150	92	96	-----
Pylon torsion, cps	---	126	---	157	170
Complex modes, cps	180	224	220	190-220	119, 225, 252
Fin first bending, cps	128	120	115	112-120	115-120

The fin first bending frequencies for the two semisubmerged store models (models A and B) and the cavity model (model C) were between 110 and 120 cps.

Each model, except model C, was accelerated to approximately $M = 1.1$ by an external booster rocket motor and was then allowed to coast to about $M = 0.85$, at which time a sustainer rocket motor, within the fuselage, fired and accelerated the model to approximately $M = 1.4$. The cavity model (model C) did not have an internal sustainer rocket motor but was propelled by a larger external booster rocket motor to approximately $M = 1.8$. A typical model-booster combination mounted on a rail-type launcher prior to the test flight is shown in figure 5. The data from these models were received continuously during each flight by using a standard NACA telemetering system. Model velocity was obtained by using CW Doppler radar, and flight-path data were obtained from SCR 584 tracking radar. The scale of these tests is shown by the Reynolds number plot in figure 6, and dynamic pressure is plotted against Mach number in figure 7. Only data from the coasting periods are used in this report.

The isolated-store models used in conjunction with this investigation and shown in figure 4 were tested by the helium-gun technique of reference 6. The Reynolds numbers for these models, based on the isolated-store model length, ranged from approximately 4×10^6 to 10×10^6 between Mach numbers of 0.8 and 1.3. All flight tests were performed at the Langley Pilotless Aircraft Research Station, Wallops Island, Va.

ACCURACY

The minimum buffet amplitudes that could be detected during these tests were estimated to be of the order of $\pm 0.05g$. This estimate is based on the width of the recorded accelerometer traces and the calibration data for the individual instruments. In most cases the total drag coefficients calculated from the longitudinal accelerometer in the model and from CW Doppler radar have been in good agreement. The maximum error in the total drag coefficient is estimated to be ± 0.01 at subsonic speeds and ± 0.005 at supersonic speeds. The maximum errors in the trim normal-force and side-force coefficients are estimated to be ± 0.02 at subsonic speeds and ± 0.01 at supersonic speeds. Mach numbers are estimated to be accurate within 2 percent at subsonic speeds and 1 percent at supersonic speeds.

PRESENTATION OF DATA

Data from flight tests of eight rocket-powered buffet research models having various arrangements of external fuselage-mounted stores are

presented herein. Drag data from helium-gun tests of three isolated store models are also presented for comparison. Many of these data have been published previously in reference 2 but are reproduced herein for comparison with more recently acquired data. The data presented herein consist primarily of trim normal- and side-force coefficients, accelerations due to buffeting, and drag coefficients at trim conditions plotted against Mach number.

Trim

Trim characteristics of all rocket-powered models are presented in figures 8 and 9. These trim data are presented primarily for reference purposes to show the range of lift and side-force coefficients at which the buffeting and drag data were obtained.

Buffeting

Buffeting is considered in this paper to be any random shaking of an aircraft or its components induced by rough or separated flow on or around the aircraft or its components. Buffeting is differentiated from flutter by the random nature of the vibrations, by the absence of evidence of coupling of structural modes at the predominant vibratory frequencies, and by the fact that the models of the present tests were designed as well as possible to be flutter-free within the Mach number range of these tests. Buffeting was differentiated from model response to gusts by the absence of appreciable undamped response of the complete model at its natural pitching and yawing frequencies and by the fact that the random vibrations that occurred on the test models occurred at altitudes and in weather conditions such that the required gust disturbances for model response were not anticipated.

Sections of actual telemeter records are reproduced in figure 10 to illustrate the buffet characteristics of all models at the Mach number for peak buffet intensity ($M = 0.92$) and at supersonic speeds ($M = 1.2$) for all models having pylon-mounted stores. The very small amplitude roughness evident on the records of models A and B (fig. 10(a)) is not an indication of buffeting but is an extraneous signal known to have been superimposed on the telemeter signal of these models.

Buffet-intensity data obtained by visual analysis of records similar to those of figure 10 for each of the test configurations are presented in figure 11 as the amplitude of the oscillating accelerations due to buffeting plotted against Mach number. Only those data measured in the transverse plane are presented herein (except in the case of model C), not because there was no buffeting in the normal plane, but, rather,

because the buffeting in the normal plane occurred at frequencies generally too high and too random to permit adequate amplitude-response corrections to the measured amplitudes. Buffeting was recorded in the normal plane of every model that experienced buffeting in the transverse plane but is believed to have been generally lower in magnitude than that in the transverse plane.

The transverse buffet intensities presented in figure 11 are the recorded values corrected for the amplitude response of both the accelerometer and the recorder at the predominant frequencies encountered. In general, these were the lower, or pylon bending, frequencies (see table in "TESTS" section) and resulted in amplitude response factors ranging from about 0.5 to 1.1. Transverse accelerations measured in the store and in the fuselage tail are presented in figure 11 to show the relative amplification of the oscillations due to structure. In all cases involving externally mounted stores the transverse acceleration in the fuselage tail was much lower than in the store and has been omitted in figure 11(c) for clarity. It should be noted that visual analysis of accelerometer records to obtain buffet intensities could only be accomplished at points where a definite frequency could be observed; thus, in some instances, particularly at supersonic Mach numbers, the data shown herein appear to be very scattered. This is a definite limitation of visual analysis and does not indicate intermittent buffeting. It is believed that the amplitudes measured at definite frequencies were the maximum amplitudes actually felt by the accelerometers.

The technique of frequency-spectrum analysis utilizing electrical machines has been applied to data from two of the configurations reported herein (models C and H). This technique did not prove useful in these particular applications and the resulting data have been omitted from this paper. It is felt that the failure of this technique to be useful in these instances was because continuous representative-sample time histories could not be obtained with the rapidly changing flight conditions of the tests and because the buffet amplitudes encountered on these models were small compared with the accelerometer calibration ranges used. This does not mean that the frequency-spectrum-analysis technique is not applicable to rocket-powered models. It does mean, however, that models for which frequency analysis of the data is desirable should be designed for this purpose by obtaining the very minimum change in flight conditions possible over the period to be analyzed and by utilizing as near full-scale instrument calibration ranges as possible.

Drag

Total drag coefficients and installation drag coefficients are plotted against Mach number in figures 12 to 14. Total drag coefficients are based on fuselage frontal area; whereas, installation drag

coefficients (the increments of drag coefficient added to the basic configuration by the store assemblies) are based on actual store frontal area. Also shown for comparison are the drag coefficients of the basic (no stores) configuration from reference 3 and of the isolated-store shapes as obtained from the helium-gun tests. Since the stores attached to the basic configuration had no fins, the estimated fin drag of the isolated-store models was subtracted from their total drag and the difference is presented herein as isolated-store drag data.

Pressures

Differential-pressure coefficients measured between the cavity and the opposite fuselage surface of model C are plotted against Mach number in figure 15. The values presented herein were obtained by fairing the telemeter records for model C in figure 10(a) and hence are from average values of differential pressure existing at a given Mach number. It may be seen that the oscillating pressures encountered were of extremely random nature with no one predominant frequency; consequently, it is not possible to analyze these data visually to obtain true oscillation amplitudes. Thus, no oscillating pressure intensities are presented.

Pressure coefficients obtained from static-pressure measurements at two points on the fuselage surface are shown in figure 16 and are compared with data from references 3 and 7 obtained for the basic configuration. In the present tests, one static-pressure orifice was located on the side of the fuselage (90° from the plane of the fuselage-cavity center lines) at approximately the maximum fuselage diameter. The other static-pressure orifice was located directly behind the cavity and between the stabilizing fins of the model. It should be noted that the side orifice near the fuselage maximum diameter was approximately 1 inch forward of the comparable orifice of references 3 and 7; hence, absolute agreement of pressure data from these stations would not be expected.

RESULTS AND DISCUSSION

Results of flight tests of eight wingless rocket-powered buffet research models having various arrangements of fuselage-mounted external stores, and results of drag studies of three isolated store models, are compared and discussed herein. These results cover a Mach number range from approximately $M = 0.7$ to $M = 1.4$.

Trim

The trim data presented in figures 8 and 9 show that no severe trim conditions or abrupt trim changes were experienced by any of the

configurations tested. In general, the trim levels were near zero throughout the Mach number range of the tests in both the normal and transverse planes. Small transonic trim changes were evidenced by most configurations in both the normal and transverse planes, but there appears to be no consistency in either the direction or magnitude of these changes.

All configurations having completely external stores (models D, E, F, G, and H) experienced zero or small positive trim normal forces at subsonic speeds. Since these models were unsymmetrical geometrically and no attempt was made to control the vertical center-of-gravity position, this positive subsonic trim condition was probably an induced effect of the store installations.

Buffeting

The basic fuselage and tail configuration used in these investigations was free of any low-lift buffeting within the Mach number range of these tests (ref. 3). Any buffeting encountered in these tests, therefore, must be caused by the addition of the external stores to the basic configuration. Data of references 3 and 8 show that low-lift buffeting resulting from airfoil section characteristics should not exist above about $M = 1.0$. It is believed that this limit can be applied to the pylons and store shapes of the present tests. Thus it is believed that the buffeting encountered on all the external stores of this investigation at supersonic speeds was induced by mutual interference between the fuselage and store assemblies.

Effect of semisubmerged stores.- No buffeting was encountered on either of two configurations having models of a large-diameter bomb shape semisubmerged in the fuselage at two different longitudinal locations (models A and B in figs. 10(a) and 11(a)). These data indicate that the large-diameter bomb-shape store was itself buffet-free throughout the Mach number range of these tests.

Effect of a semisubmerged store cavity.- Mild buffeting was encountered on the model with the bomb cavity (model C) throughout the test Mach number range from approximately $M = 0.7$ to $M = 1.8$. This configuration represents model A after release of the semisubmerged store. Buffeting of this model was indicated by both normal and transverse accelerometers within the fuselage and by differential pressures measured within the cavity (fig. 10(a)). Accelerometer data show maximum structural response at the stabilizing-fin first bending frequency; whereas the pressure data were of extremely random frequency (none predominant). Although accurate amplitude-response characteristics of the pressure-measuring systems are not known, it is believed that the oscillating pressures were no greater than the actual recorded values

and that the maximum oscillating pressure encountered on this model was of the order of ± 0.5 lb/sq in. Static pressure measured on the fuselage surface at two stations showed no indication of oscillating pressures. These data indicate that the mild buffeting encountered on this model was a local phenomenon associated with turbulent flow within the cavity. It is interesting to note that model A, which could represent a fighter-bomber configuration with a semisubmerged bomb, appears to be good from the buffet standpoint until such time as the bomb is released (model C), after which time its performance might be reduced due to buffeting within the cavity exposed by the bomb release.

Effect of vertical store location.- Buffet-intensity data from tests of three configurations having the same store shape at the same longitudinal location (fig. 11(b)) indicate that vertical store location is a major factor affecting the buffeting of fuselage-mounted external stores. Buffeting was encountered throughout the test Mach number range on both configurations having completely external stores (models D and E). Note that the store located tangent to the fuselage (model D) experienced buffeting several times as severe as that encountered by the pylon-mounted store (model E) at transonic speeds. Since this store shape was buffet-free on model A, and since the buffeting was much more severe on the tangent-mounted store than on the pylon-mounted store, it appears that local interference between the fuselage and store assembly was the predominant factor in the observed buffeting. It is further evident that the presence of the thin pylon on model E was of much less importance than the proximity of the fuselage and store. These data indicate that a low-fineness-ratio smooth-contoured store carried in a semisubmerged location probably would not affect seriously the buffet characteristics of an aircraft; whereas, if the same store is carried externally on the fuselage, it should be pylon mounted away from the fuselage.

Effect of external-store shape.- Buffet-intensity data from tests of three configurations having different store shapes at comparable vertical and longitudinal fuselage locations show that the large-diameter bomb shape (model F) buffeted much more severely than either the DAS shape (model G) or the WADC shape (model H). The variations of store shape in these tests appear to have less effect on the measured buffet intensity than did the variation of vertical location previously noted. Data from models G and H indicate that the WADC shape buffeted less severely than the DAS shape, but the general level of both models is so low that this comparison is questionable. Data from these tests are inconsistent with any one shape factor such as nose bluntness or after-body curvature. It is believed that the more severe buffeting of model F, as compared with the other shapes tested, can be attributed primarily to interference effects associated with the relatively low fineness ratio of the large-diameter bomb shape. Since models F and G had similar pylons whereas models G and H had very dissimilar pylons, and, since buffeting attributable directly to pylon section would be

expected to be more severe on the 10-percent-thick pylon (model G) than on the 6-percent-thick pylon (model H), it is indicated that any effects of pylon section on the observed buffeting were probably negligible for the previous comparison of store shapes.

Effect of pylon section.- Comparison of data from tests of models E and F of figures 11(b) and 11(c) indicates, however, that pylon thickness or section, or both, may have a significant effect on the buffeting of some fuselage-mounted stores. The difference observed between these two models can be attributed only to the pylons since all other geometry was the same. The model having the 10-percent-thick smooth-contoured pylon (model F) buffeted more severely than the model having the 4-percent-thick modified-flat-plate pylon (model E). The increase in buffet intensity attributable to pylon section is believed to be primarily an effect of thickness of the pylon section, and, since the effect appears to be nearly constant at both transonic and supersonic speeds, is believed to be primarily a result of the strengthening of the existing conditions.

Drag

It has been assumed, for comparison of data from these tests, that the direct contributions of the pylons to the drag of the configurations were negligible relative to the installation-drag increments, and no adjustments for pylon drag have been made in the data presented herein. All drag data presented herein were measured at trim conditions; however, the general trim levels were sufficiently low that drag due to lift can be neglected.

Effect of semisubmerged stores.- Drag-coefficient data from the two semisubmerged store configurations (models A and B in fig. 12) indicate that the longitudinal location of the semisubmerged store of these tests has little effect on the drag of a configuration at Mach numbers above about $M = 1.1$. This result is in general agreement with the data of reference 1 where the three positions investigated showed only small differences in drag coefficient. The store of reference 1 was the DAS shape; whereas the store of the present test was a large-diameter bomb shape. Thus, the major effects of semisubmerged store location appear to be largely independent of store shape at supersonic speeds.

Installation drag coefficients are compared with the isolated-store drag coefficients in figure 12(b). Note that near $M = 1.1$, little or no interference drag was present for either store location; whereas severe interference at transonic Mach numbers is evident for the forward location.

Effect of semisubmerged store cavity.- Data from model C (fig. 12) show that the cavity for carrying a semisubmerged large-diameter bomb

shape caused more drag throughout most of the test Mach number range than did the store in place (model A). This result agrees with data of reference 1 which shows higher drag for a cavity at all test locations than with a semisubmerged store in place.

Pressure data measured within the cavity (fig. 15) indicate that the higher drag experienced with the cavity is an effect of the local flow within the cavity. Note that all differential pressures measured between the cavity and the opposite fuselage surface are of such sign as to contribute to the drag of the model. Since the static pressures on the fuselage surface show only minor variations from pressures measured on the basic fuselage (refs. 3 and 7) it appears that the large drag contribution was local within the cavity.

Effect of vertical store location.- Data from tests of three configurations (models A, D, and E in fig. 13) having the same store shape mounted at the same longitudinal location show that vertical store location is a major factor contributing to the drag of fuselage-mounted external stores. It is immediately apparent that the semisubmerged location (model A) offers the smallest drag per unit of exposed frontal area of any of the locations tested. Also apparent is the very high drag of the store mounted tangent to the fuselage (model D). It may be seen that even with a thin pylon added to model D to move the store away from the fuselage (model E) a significant reduction in total drag was obtained. In figure 13(b), it is seen that this reduction amounted to approximately a third of the interference increment at supersonic speeds (about 20 percent of the total installation drag). Thus it is indicated that the drag of a configuration carrying fuselage-mounted external stores probably can be reduced by either partial submergence of the store or by mounting the store away from the fuselage on a thin pylon support. It should be noted, however, that the data herein can only be applied qualitatively to configurations other than the specific configurations of these tests since interference appears to be a predominant factor.

Effect of external-store shape.- Drag coefficients from tests of three configurations having different external-store shapes mounted at comparable vertical and longitudinal locations (models F, G, and H in fig. 14) show that the DAS shape (model G) is appreciably better at supersonic speeds than either the WADC shape (model H) or the large-diameter bomb shape (model F). The lower installation drag coefficients of the DAS shape at supersonic speeds (fig. 14(b)) are believed to result from the lower isolated drag of this shape which in turn is thought to be a result of the higher fineness ratio and sharper nose of the DAS store. It should be remembered that any effects due to the differences in pylon sections were assumed to be negligible for these comparisons.

In figure 17, the installation drag at sea-level standard conditions per unit of store volume is shown for each store shape tested. This parameter may be interpreted as a measure of the relative efficiencies of the different assemblies. Again, the DAS shape appears to be better at supersonic speeds although the WADC shape may be slightly better below about $M = 0.93$. Note that the efficiency (installation drag per unit volume) appears to be largely a function of store fineness ratio.

Effect of pylon section.- Comparison of model E (fig. 13) with model F (fig. 14) shows that the absolute effect of pylon section on the drag of an external-store installation may be appreciable. It may be seen that changing from the 4-percent-thick flat-plate pylon of model E to a pylon having a 10-percent-thick airfoil section (model F) increased the installation drag between Mach numbers of about 0.85 and 1.2 (maximum of about 15 percent near $M = 1.0$). The data indicate, however, that the effects of pylon section were not constant and were less than 15 percent over most of the Mach number range (very small near $M = 1.2$). Note, however, that these effects cannot be evaluated closer than about 30 percent near $M = 1.0$ and 100 percent near $M = 1.2$ because of the quoted possible inaccuracies of the total-drag data. Thus, the above evaluation of pylon section effects must be considered only qualitative.

The maximum value of total pylon drag, exclusive of interference, estimated in reference 1 for pylons similar to those of the present tests was of the order of 10 percent of the drag of the isolated DAS store, but the difference shown in reference 1 for the two pylon sections was very small relative to the isolated-store drag. Thus it appears that the pylon contributed more drag in the present tests than would normally be predicted. However, because of the possible inaccuracies mentioned above, no attempt is made to evaluate these additional, or interference, effects.

Note that the above comparison between models E and F represents the most radical difference of pylon section existing in the present tests. It is therefore believed that the previous assumption of negligible pylon drag relative to the other installation-drag increments was valid for purposes of the comparisons of this paper.

General discussion of drag characteristics.- Large installation-drag increments were associated with the fuselage-mounted external-store assemblies of this investigation throughout the test Mach number range. This installation drag contained large interference-drag increments which, at transonic speeds, were several times larger than the drag of the store alone. The total-drag data presented herein show that in no case was the drag-rise Mach number changed appreciably by the addition of external stores to the basic configuration. In all cases except

models B and C, the peak total drag occurred at lower Mach numbers than the peak drag of either the isolated store or the basic configuration; this fact indicates that the build-up of interference drag was more rapid than the drag rise of the configuration components. It should be noted here that the magnitude of the peaks of the installation-drag curves were obtained from points on the steep slope of the configuration drag rise and hence may be of reduced accuracy. However, it is believed that the transonic trends shown herein are reliable.

Figure 18 was prepared in an attempt to consolidate and compare the interference-drag increments present in these tests. Here, the ratio of installation drag coefficient to isolated-store drag coefficient is plotted against Mach number, and, since it is a ratio, unity indicates no interference. Note, in all cases except for models B and G, the severe peaks at transonic speeds. Perhaps even more interesting is the tendency of the similar installations to approach the same supersonic value; that is, drag ratios of the semisubmerged store assemblies approached a ratio of 1 (no interference), whereas the drag ratios of all the pylon-mounted stores approached a ratio somewhat less than 2 (interference equal to store drag). The implications of these characteristics, however, are not clear in detail. The longitudinal location used in the present tests of pylon-mounted stores is believed to be about the worst possible from the drag standpoint. Thus, a limit to the magnitude of interference drag obtainable near $M = 1.2$ may exist and may be proportional to the drag of the isolated-store shape.

SUMMARY OF RESULTS

An investigation of the buffet and drag characteristics of several finless external stores mounted on the fuselage of a wingless rocket-powered research model has been conducted over a Mach number range from approximately 0.7 to 1.4. Results of this investigation are summarized as follows:

No severe or abrupt trim changes were evidenced by any of the external-store configurations investigated. Low-lift buffeting was encountered on all test configurations having completely external fuselage-mounted stores throughout the test Mach number range. No buffeting was encountered on two configurations having a semisubmerged bomb shape. Severe store buffeting was encountered on a configuration having a large-diameter bomb-shape store mounted tangent to the fuselage. A similar configuration with the store mounted on a 10-percent-thick pylon encountered much less severe store buffeting than did the tangent-mounted store but buffeted more severely than did a similar configuration having a 4-percent-thick pylon. Both the Douglas Aircraft Company, Inc., and Wright Air Development Center shapes experienced only mild store buffeting within the test Mach number range.

Large installation-drag increments were associated with the fuselage-mounted external-store assemblies of this investigation throughout the test Mach number range. This installation drag contained large interference-drag increments which, at transonic speeds, were several times larger than the drag of the store alone. The cavity for carrying a semisubmerged bomb shape caused more drag than the bomb-shape store in position. A DAS shape had appreciably lower supersonic installation drag than either a WADC shape or a large-diameter bomb shape.

These results indicate that low-lift buffeting and large drag increments can be induced by mutual interference between a fuselage and external-store assembly at both transonic and supersonic speeds. These data also indicate that interference and its associated buffeting and drag effects are aggravated by fuselage and store proximity and by pylon thickness. Drag increments due to interference of a fuselage and external-store assembly similar to those of the present tests may approach values of the order of the drag of the store alone at supersonic speeds; at transonic speeds, the drag due to interference may be several times the store-alone drag. Of the configurations tested, a semisubmerged store arrangement appears best from both the buffeting and supersonic interference-drag standpoint; however, release of such store would probably result in performance penalties because of buffeting and high drag caused by the exposed cavity. A location behind the fuselage maximum diameter appears best for a semisubmerged store at transonic speeds. Effects of pylon section and thickness on the drag of a configuration having fuselage-mounted external stores appears to be generally small relative to the total installation effects; however, pylon thickness can have an appreciable effect on both interference buffeting and drag.

Langley Aeronautical Laboratory,
National Advisory Committee for Aeronautics,
Langley Field, Va., September 13, 1954.

REFERENCES

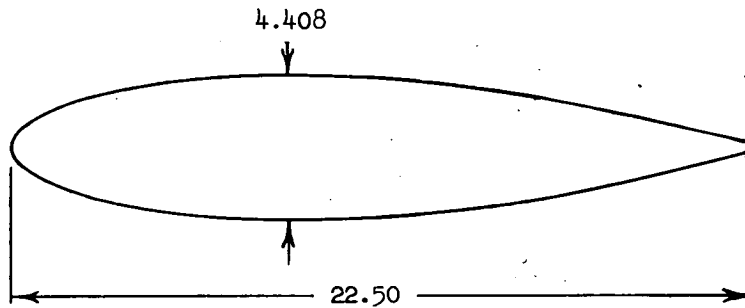
1. Hoffman, Sherwood, and Wolff, Austin L.: Effect on Drag of Longitudinal Positioning of Half-Submerged and Pylon-Mounted Douglas Aircraft Stores on a Fuselage With and Without Cavities Between Mach Numbers 0.9 and 1.8. NACA RM L54E26, 1954.
2. Mason, Homer P.: Effects of External Store Mounting on the Buffet, Trim, and Drag Characteristics of Rocket-Powered Fuselage and Store Combinations Between Mach Numbers of 0.7 and 1.4. NACA RM L53J22, 1953.
3. Mason, Homer P., and Gardner, William N.: An Application of the Rocket-Propelled-Model Technique to the Investigation of Low-Lift Buffeting and the Results of Preliminary Tests. NACA RM L52C27, 1952.
4. Muse, T. C., and Kasari, E. B.: Wind Tunnel Tests of the Douglas Aircraft Store With Various Fins. Rep. No. ES 21198, Douglas Aircraft Co., Inc., July 15, 1948.
5. Dugan, James C.: External Store Development. Memo. Rep. No. WCNSR-43019-1-1, Wright Air Dev. Center, U. S. Air Force, Aug. 31, 1951.
6. Hall, James Rudyard: Comparison of Free-Flight Measurements of the Zero-Lift Drag Rise of Six Airplane Configurations and Their Equivalent Bodies of Revolution at Transonic Speeds. NACA RM L53J21a, 1954.
7. Mason, Homer P.: Low-Lift Buffet Characteristics Obtained From Flight Tests of Unswept Thin Intersecting Surfaces and of Thick 35° Sweptback Surfaces. NACA RM L52H12, 1953.
8. Humphreys, Milton D.: Pressure Pulsations on Rigid Airfoils at Transonic Speeds. NACA RM L51I12, 1951.

TABLE I
DESCRIPTION OF EXTERNAL-STORE ASSEMBLIES

Symbol	Model	Store	Area of store, S_s , sq ft	Pylon section	Pylon length, in.	Pylon chord, in.	Total model weight, lb
	A	Large-diam. bomb shape	0.061	Semisubmerged store, forward position			62.70
	B	Large-diam. bomb shape	.061	Semisubmerged store, rearward position			63.13
	C	Large-diam. bomb shape	-----	Semisubmerged store removed			67.25
	D	Large-diam. bomb shape	.106	Tangent store			67.00
	E	Large-diam. bomb shape	.106	Modified flat plate, 4-percent-thick	2.204	5.62	66.30
	F	Large-diam. bomb shape	.106	NACA 66A010	2.204	5.62	63.70
	G	DAS shape	.0979	NACA 66A010	2.12	9.08	67.69
	H	WADC store shape	.0979	Douglas hook shackle, ^a 3 hook shackle, 6-percent-thick	2.12	8.21	77.55

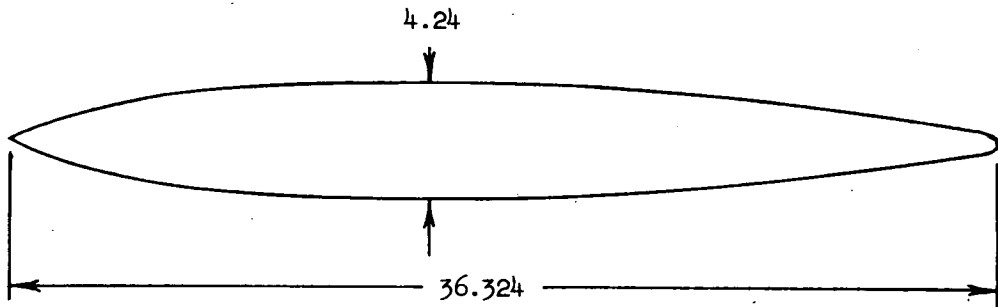
^aSee reference 5.

TABLE II
 COORDINATES OF
 LARGE-DIAMETER BOMB SHAPE



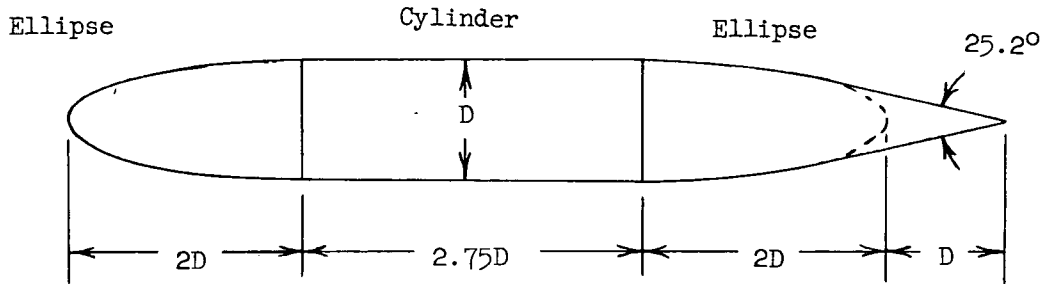
Station	Radius
0	0
.0471	.2101
.0942	.2990
.2349	.4783
.4710	.6834
1.1775	1.0906
2.3549	1.5217
3.5330	1.8049
4.7099	1.9943
5.8874	2.1142
7.0648	2.1801
8.2423	2.2034
8.4375	2.2038
9.6010	2.1871
10.7645	2.1370
11.9279	2.0538
13.0914	1.9385
14.2549	1.7927
15.4184	1.6186
16.5818	1.4194
17.7453	1.1984
18.9389	.9553
20.0727	.7087
21.2358	.4503
22.3321	.2057
22.5000	0
L.E. radius 0.4537 T.E. radius 0.2099	
Note: Afterportion is faired with straight line to remove cusp.	

TABLE III
COORDINATES OF DAS SHAPE



Station	Radius
0	0
.706	.344
2.724	1.042
3.733	1.276
4.742	1.459
5.751	1.604
6.760	1.724
7.769	1.826
8.778	1.915
9.787	1.992
10.796	2.056
11.805	2.101
12.814	2.119
15.438	2.119
18.061	2.119
19.070	2.111
20.079	2.088
21.088	2.051
22.097	2.000
23.106	1.937
24.115	1.862
25.124	1.775
26.133	1.679
27.142	1.574
28.151	1.461
29.160	1.341
30.169	1.216
31.178	1.086
32.187	.952
33.196	.816
34.003	.706
34.811	.592
35.618	.439
36.324	0

TABLE IV
 COORDINATES OF WADC STORE SHAPE



Station	Radius
0	0
.184	.439
.553	.753
1.106	1.046
1.658	1.259
2.027	1.377
2.948	1.606
3.685	1.748
4.791	1.908
5.712	2.003
6.633	2.068
7.555	2.106
8.476	2.119
20.130	2.119
21.051	2.106
21.972	2.068
22.894	2.003
23.815	1.908
25.657	1.606
26.579	1.375
27.500	1.046
28.421	.439
28.606	0

Note: Tail cone is tangent to ellipse with its vertex at store station 32.844.

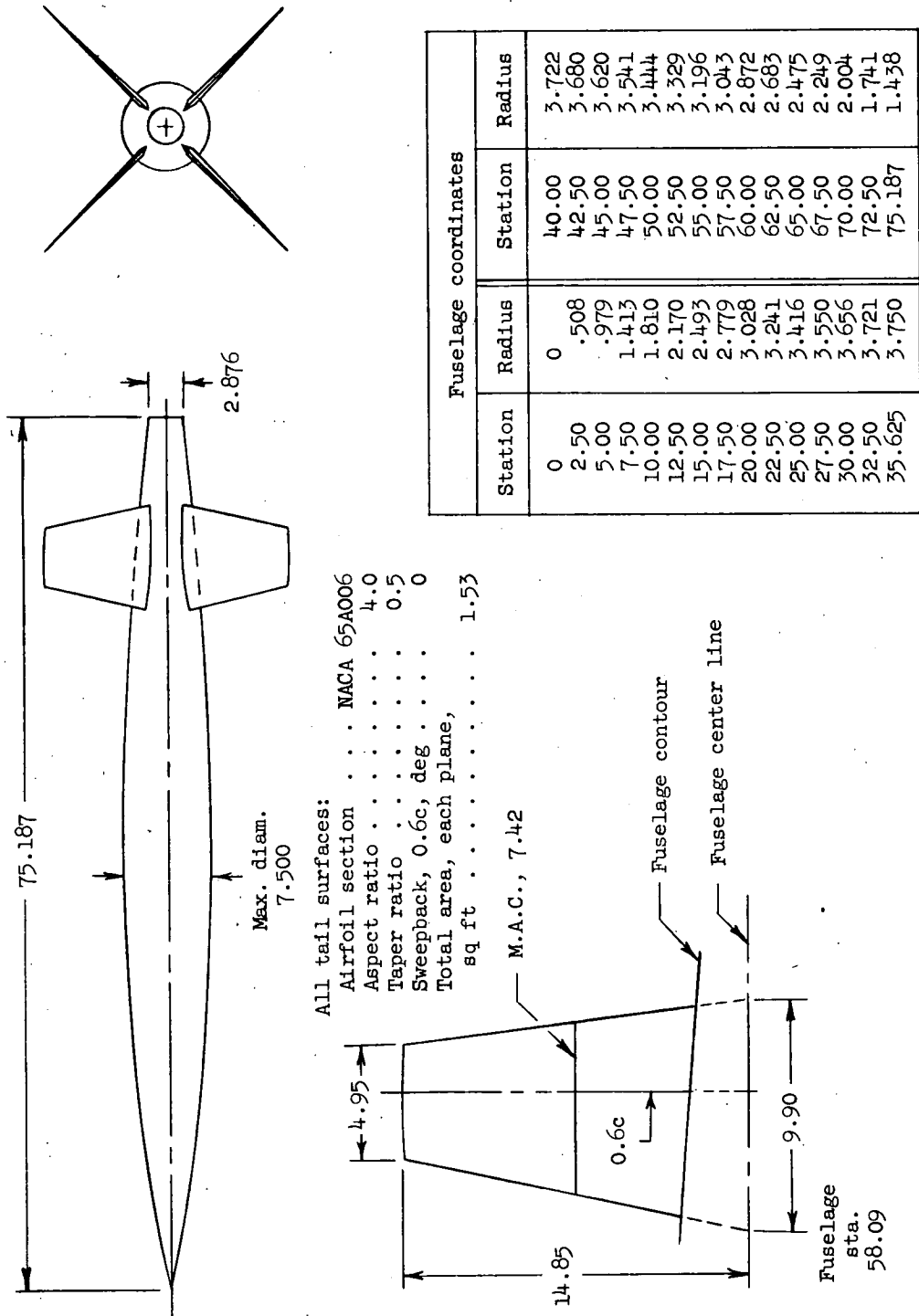
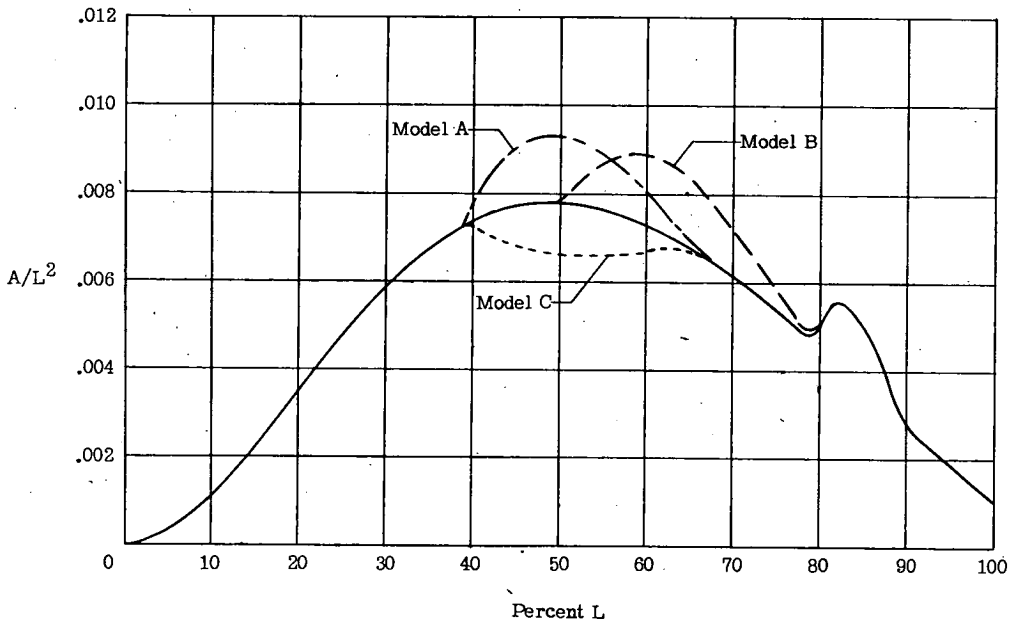
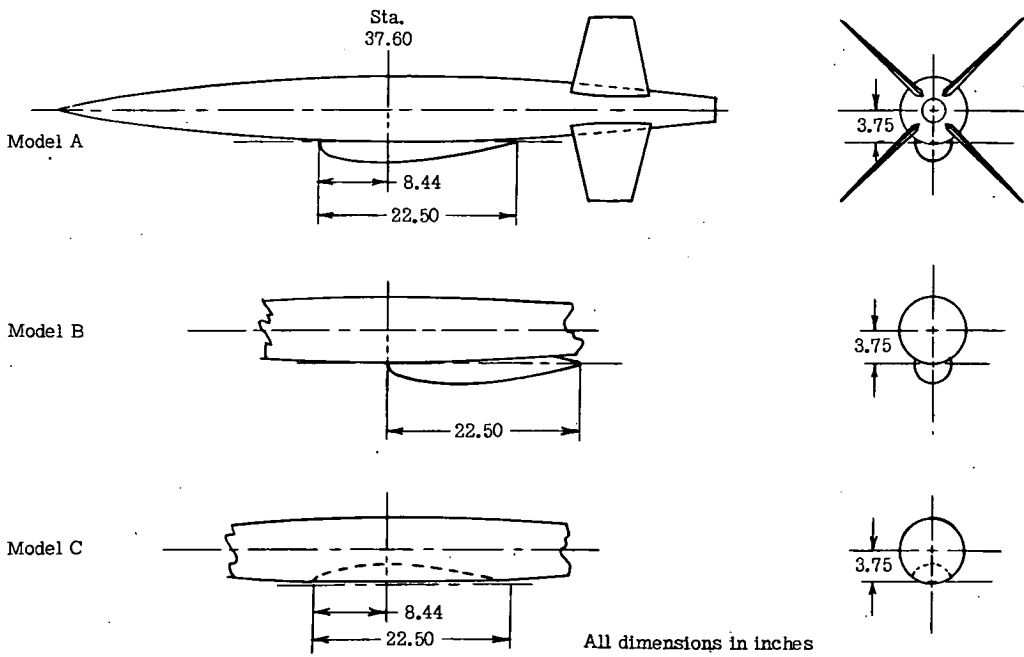
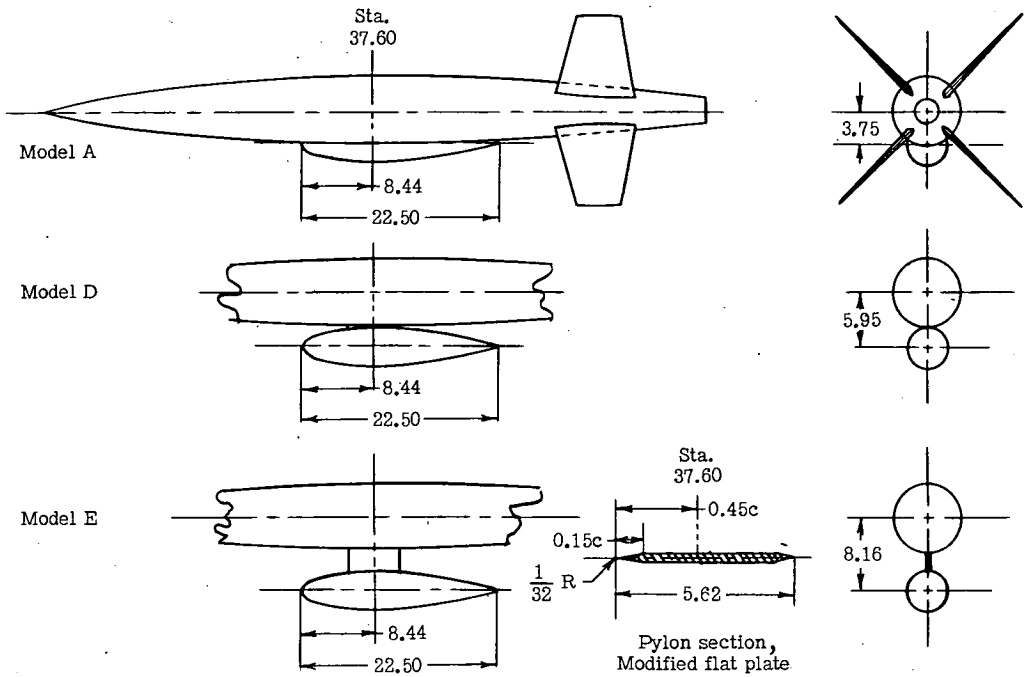


Figure 1.- Basic fuselage-tail configuration used for investigation of fuselage-mounted external stores. All dimensions are in inches.

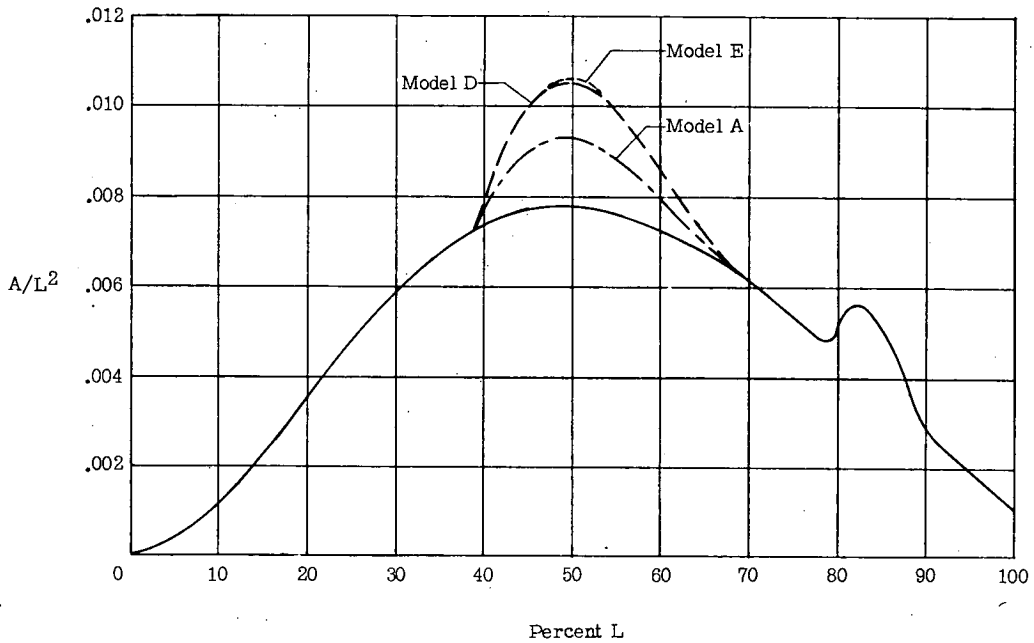


(a) Configurations employing a semisubmerged store at two longitudinal locations.

Figure 2.- Location of external stores on the test models and the longitudinal distribution of cross-sectional area of each configuration.

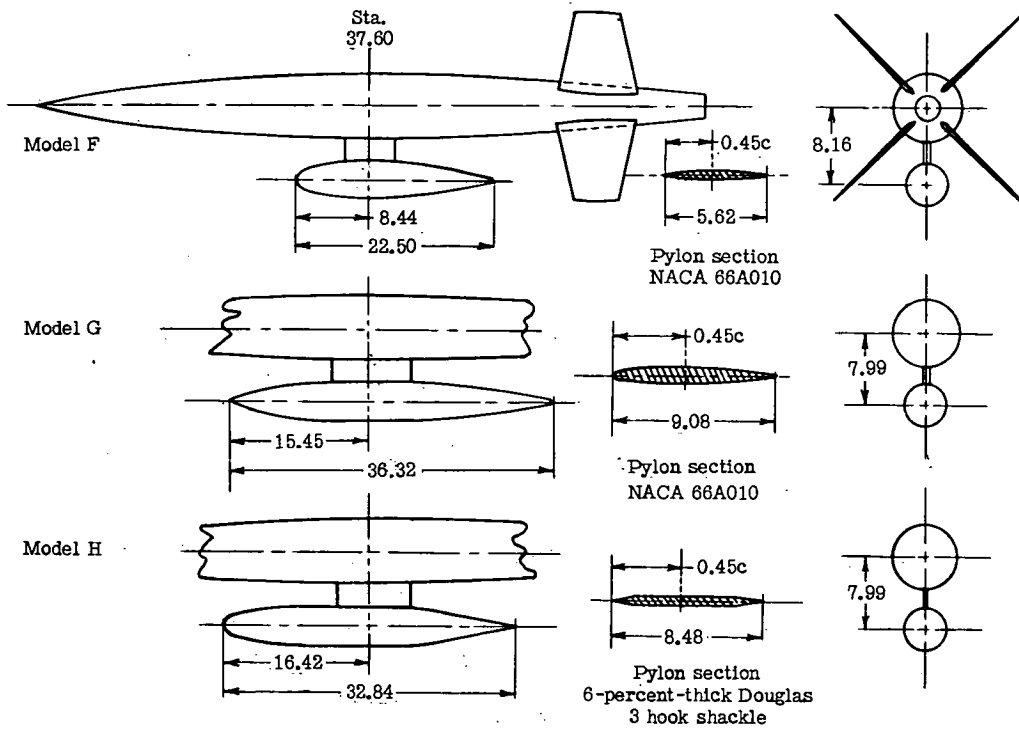


All dimensions in inches



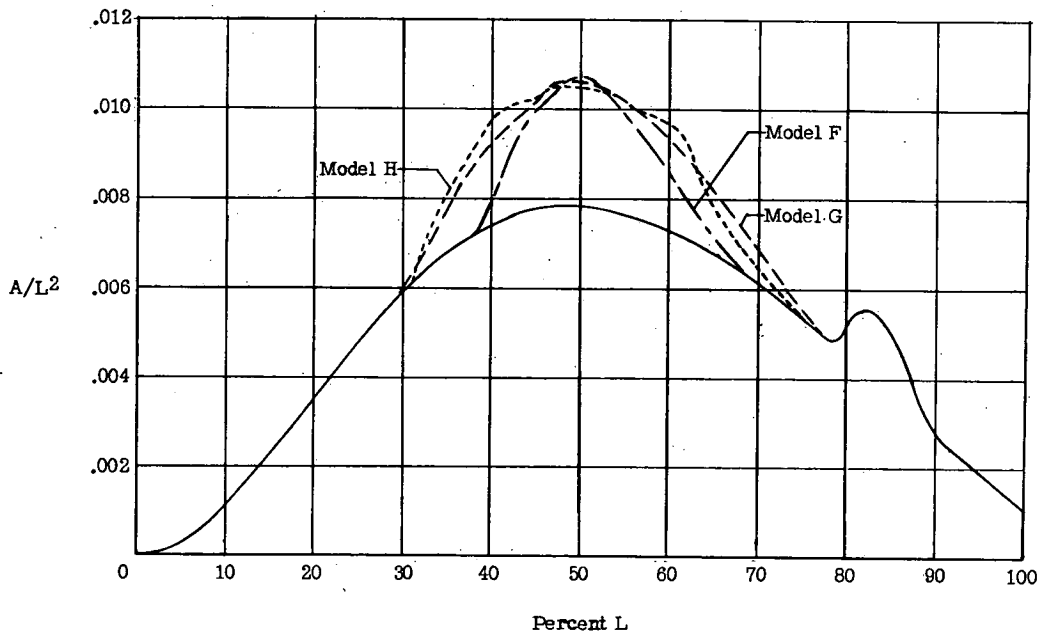
(b) Configurations employing external stores at three vertical locations.

Figure 2.- Continued.



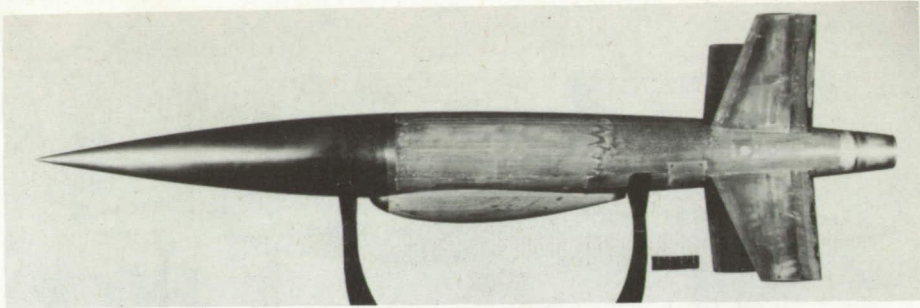
All dimensions in inches

Note: 0.45c of pylon at Sta. 37.60

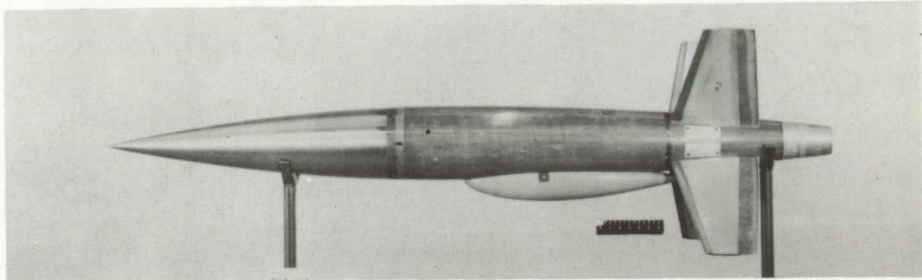


(c) Configurations employing three pylon-mounted external-store shapes.

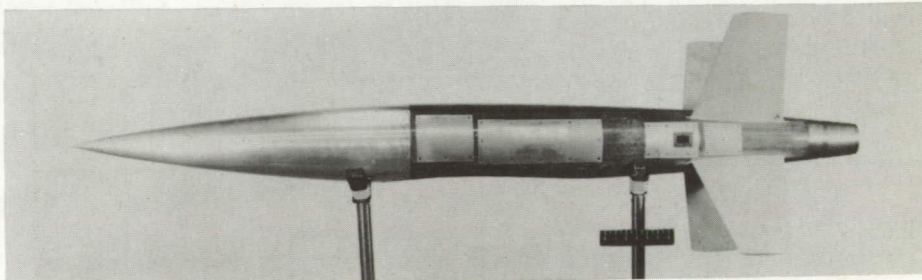
Figure 2.- Concluded.



Model A



Model B



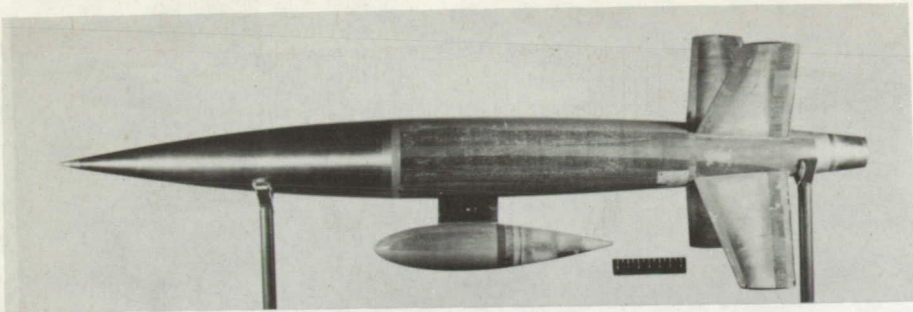
Model C



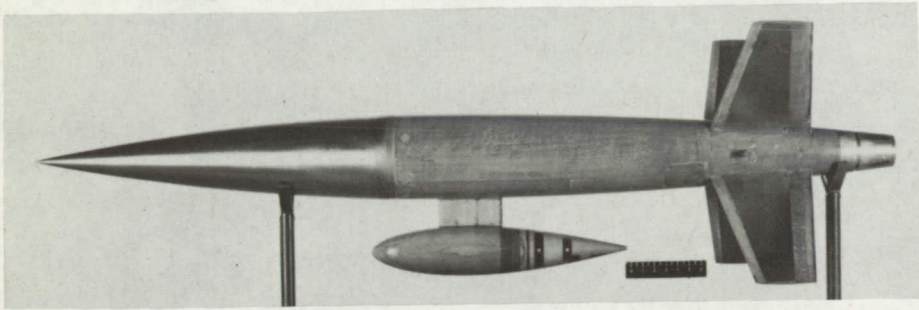
Model D

L-85673

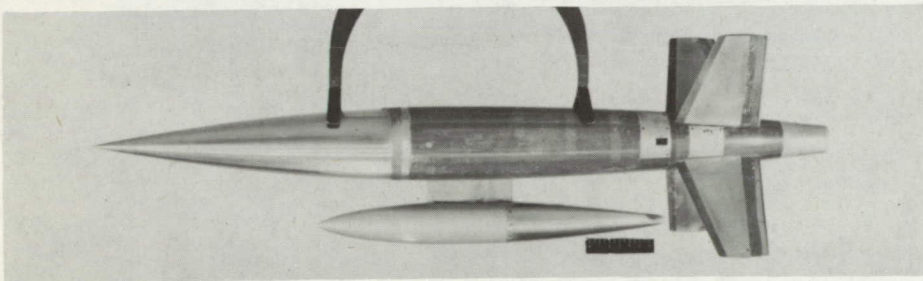
Figure 3.- Photographs of external-store configurations investigated.



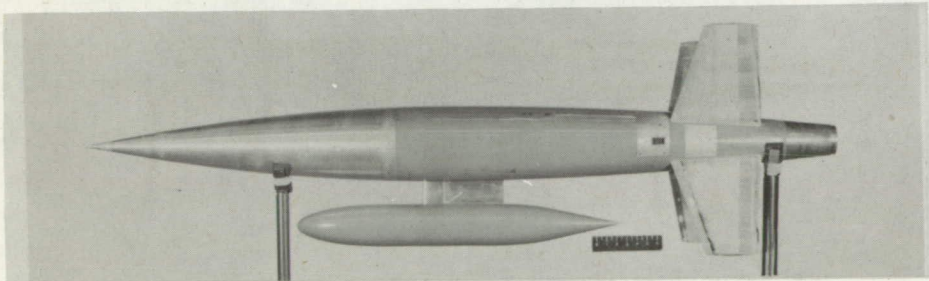
Model E



Model F



Model G



Model H

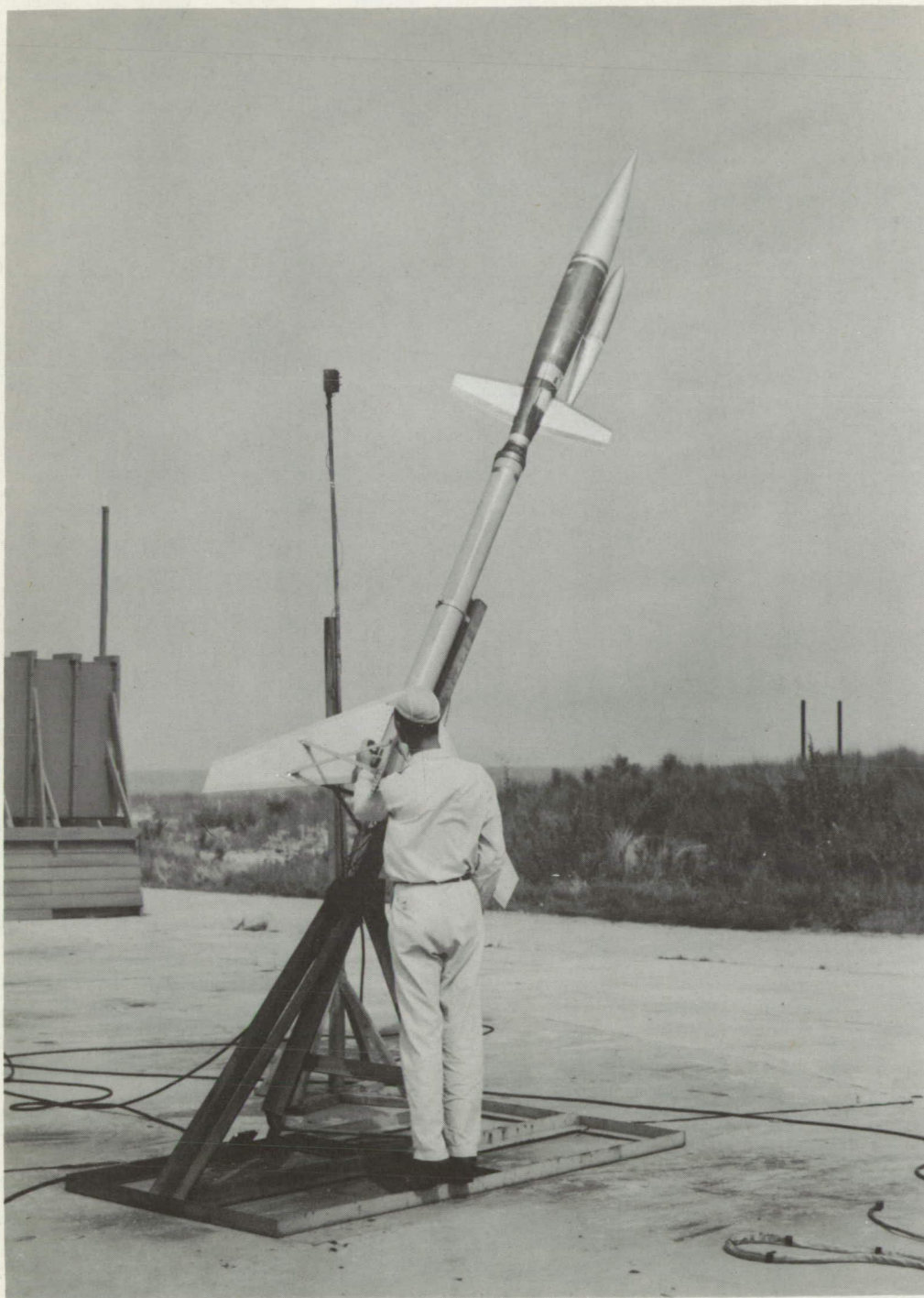
Figure 3.- Concluded.

L-85674



Figure 4.- Models used in helium-gun tests.

L-85675



L-81348.1

Figure 5.- Photograph of typical rocket model on the rail launcher.

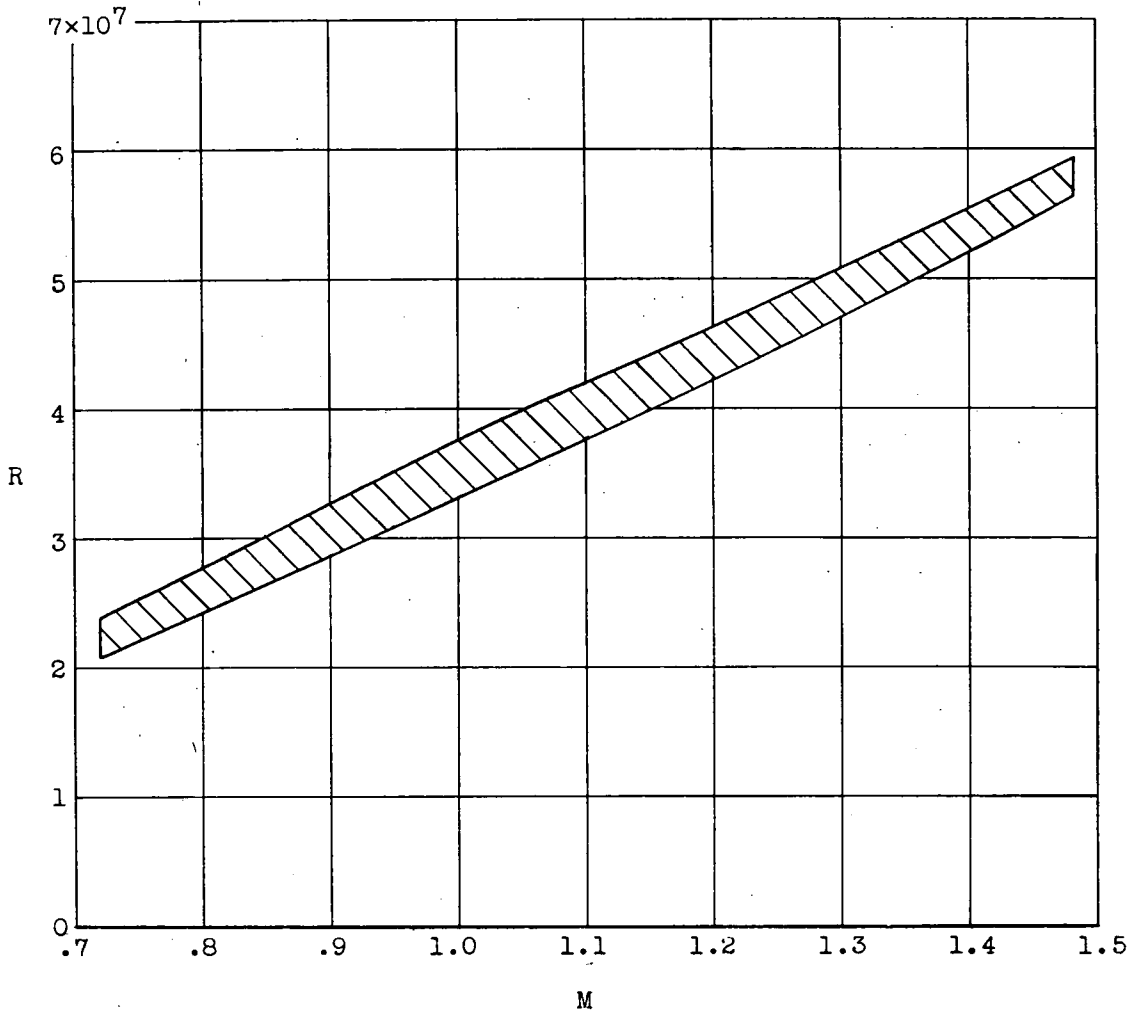


Figure 6.- Variation of Reynolds number, based on fuselage length, with Mach number.

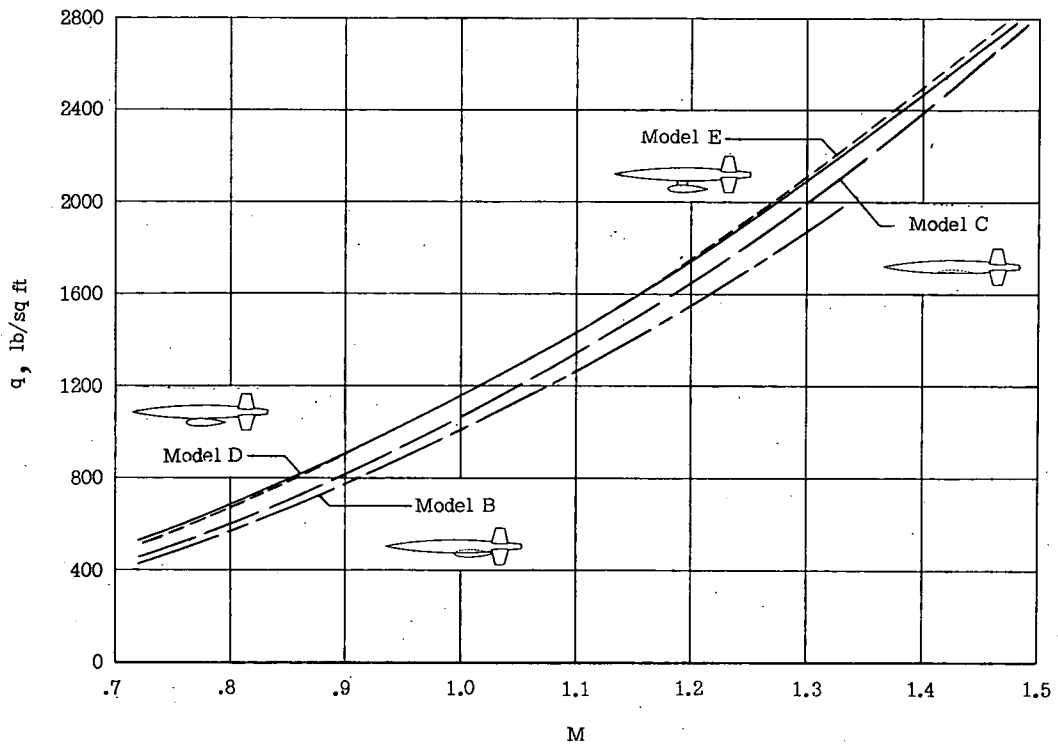
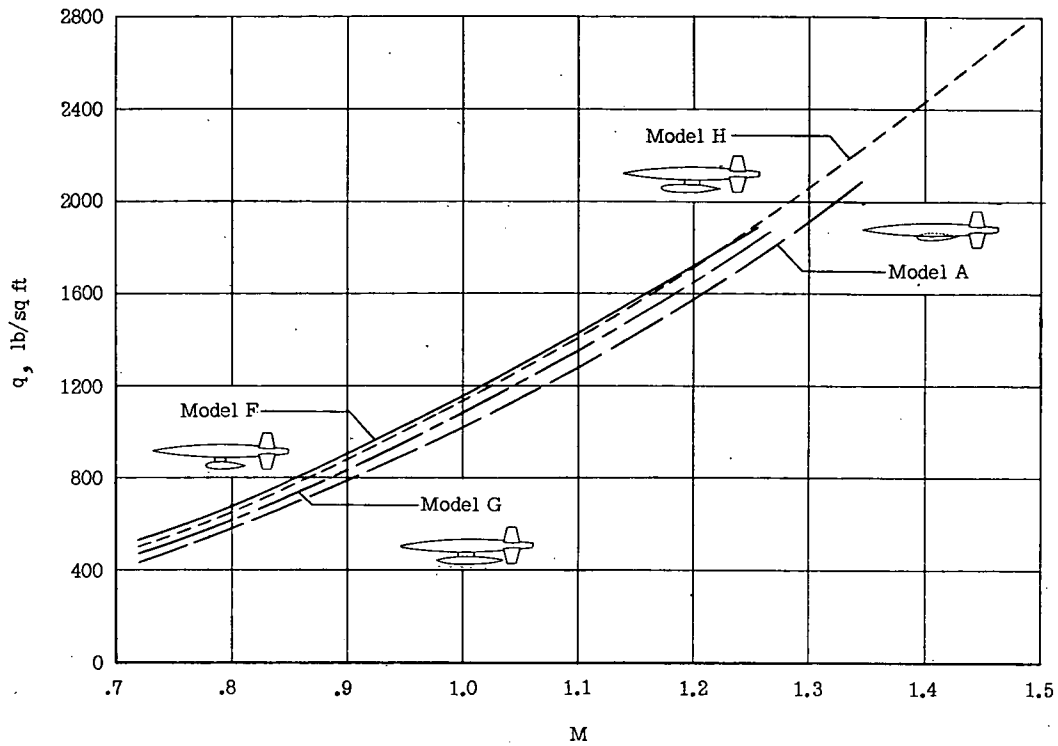


Figure 7.- Variation of dynamic pressure with Mach number.

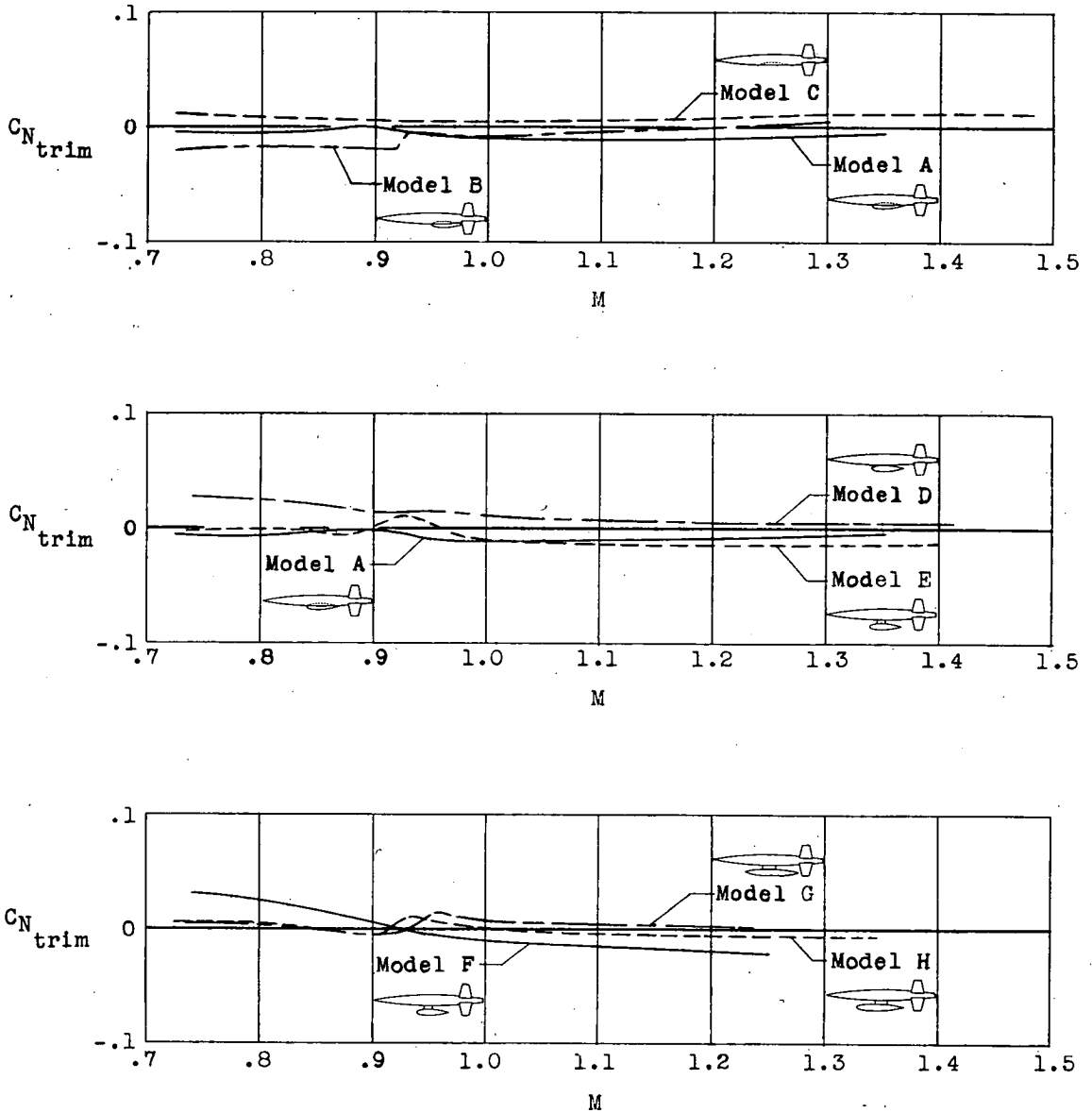


Figure 8.- Variation of $C_{N_{trim}}$ with Mach number for all models.

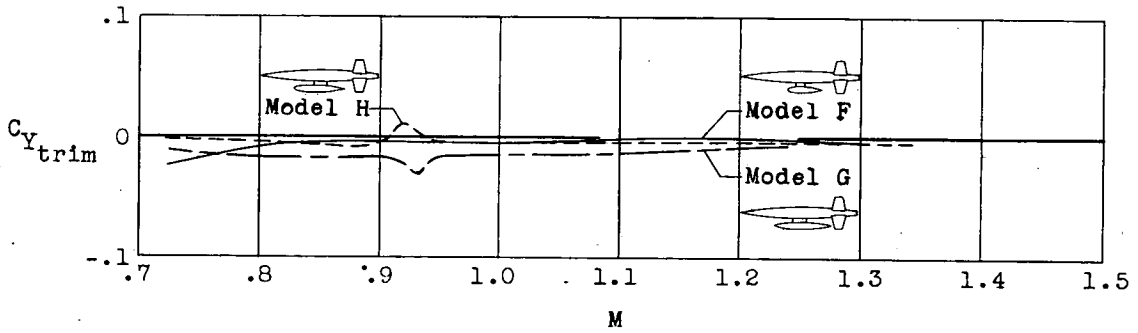
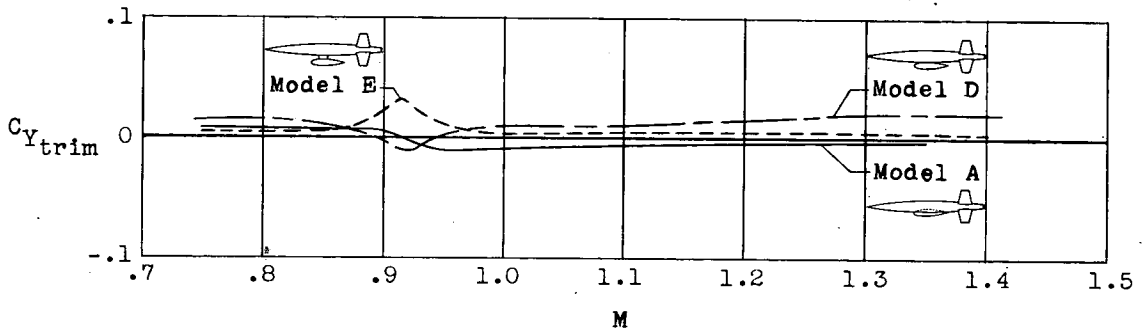
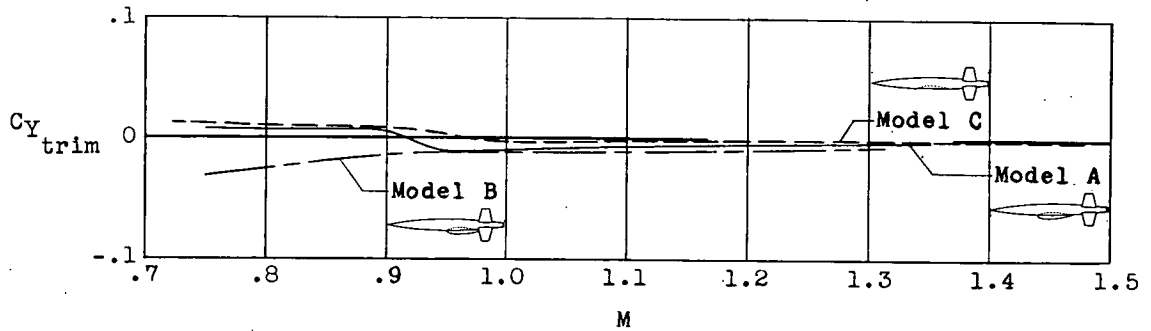
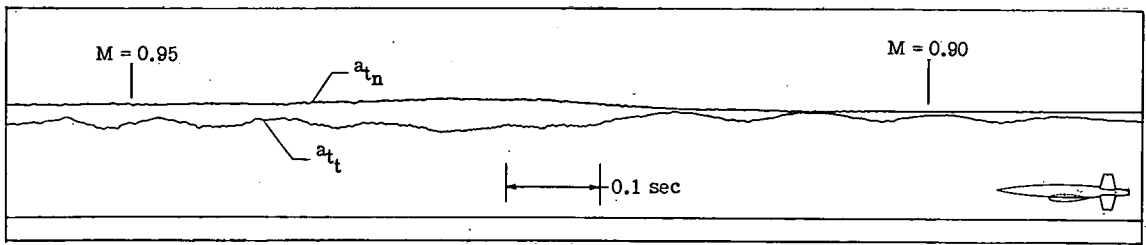
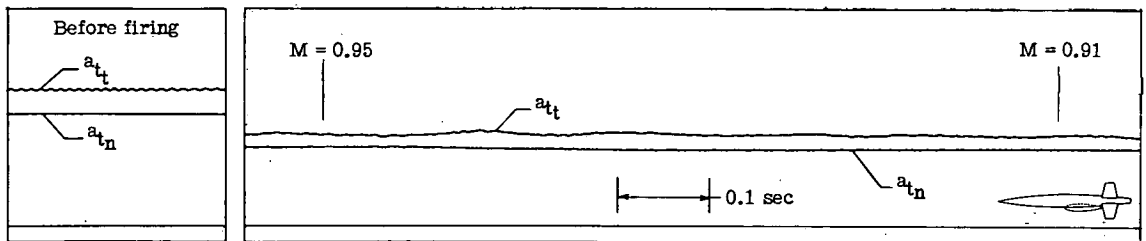


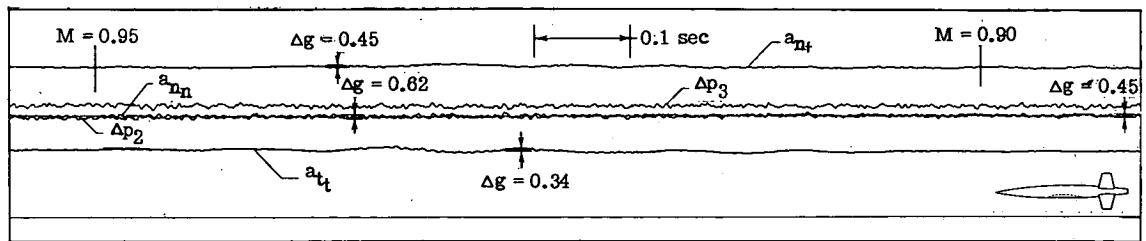
Figure 9.- Variation of $C_{y_{trim}}$ with Mach number for all models.



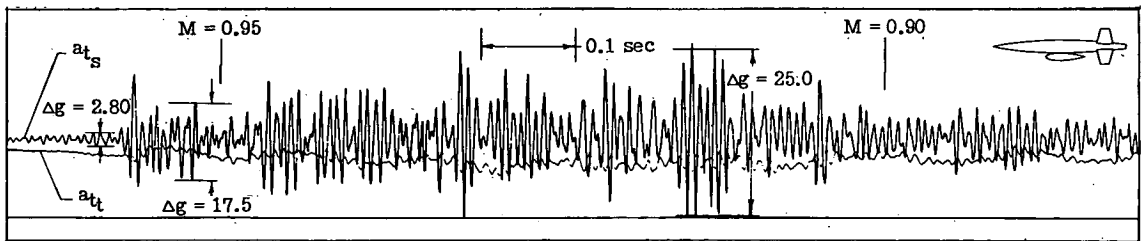
Model A



Model B



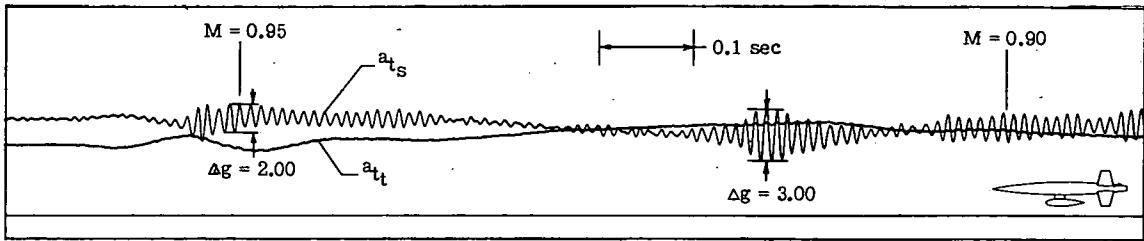
Model C



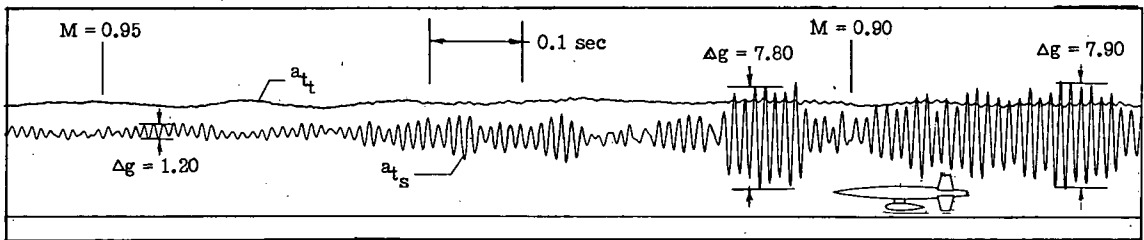
Model D

(a) Near transonic speeds for all models.

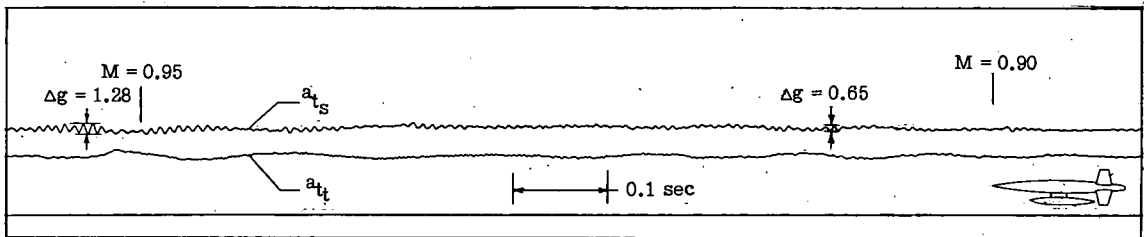
Figure 10.- Portions of telemeter record showing accelerometer traces of buffeting.



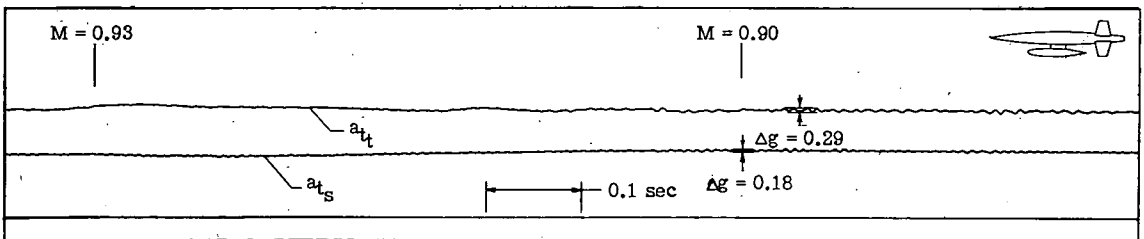
Model E



Model F



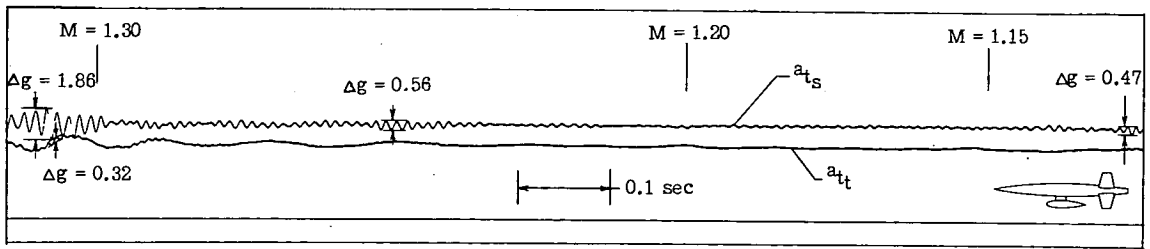
Model G



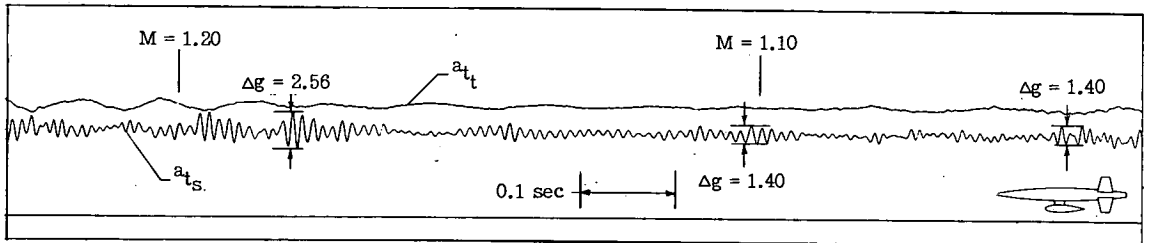
Model H

(a) Concluded.

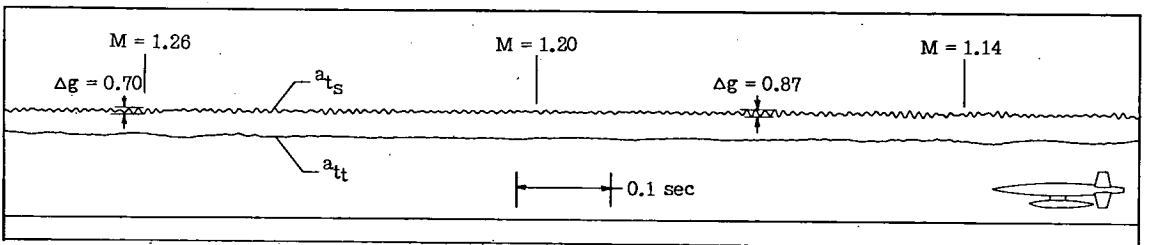
Figure 10.- Continued.



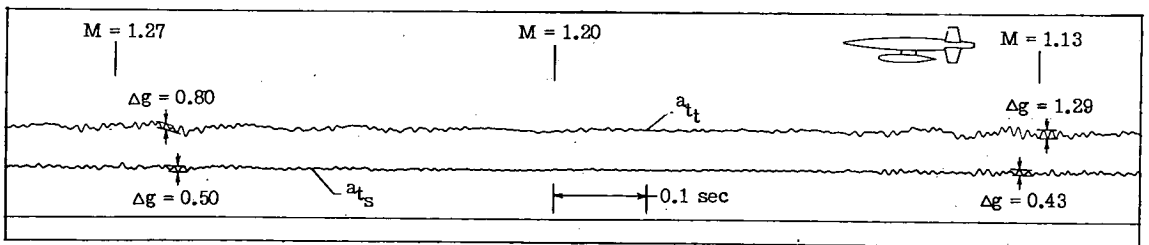
Model E



Model F



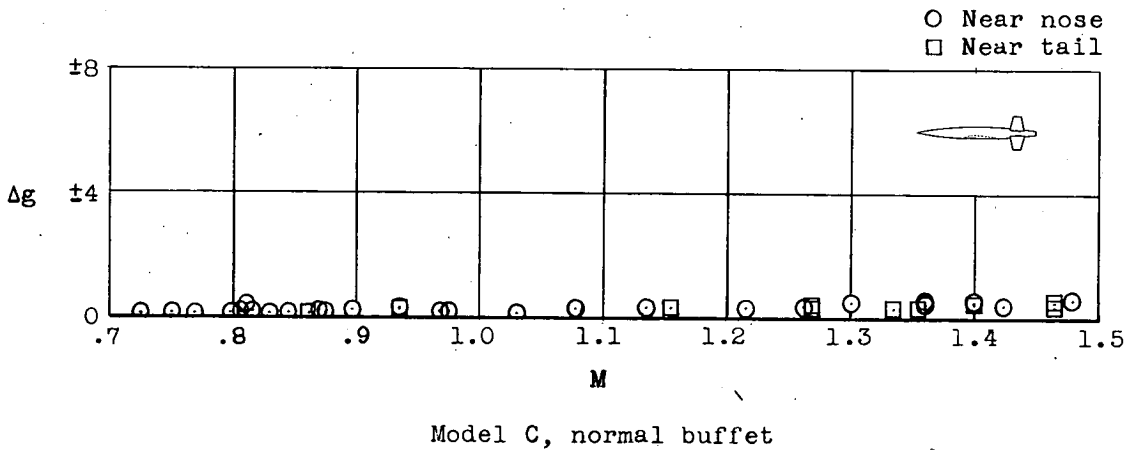
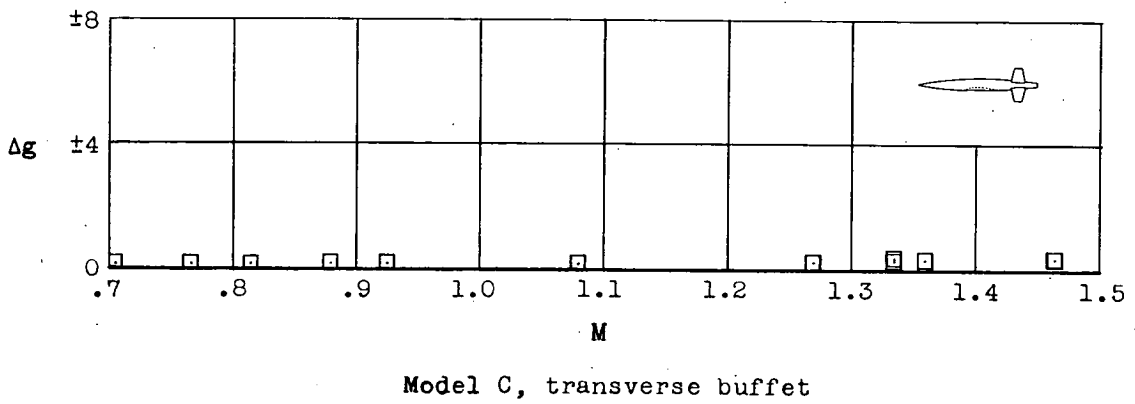
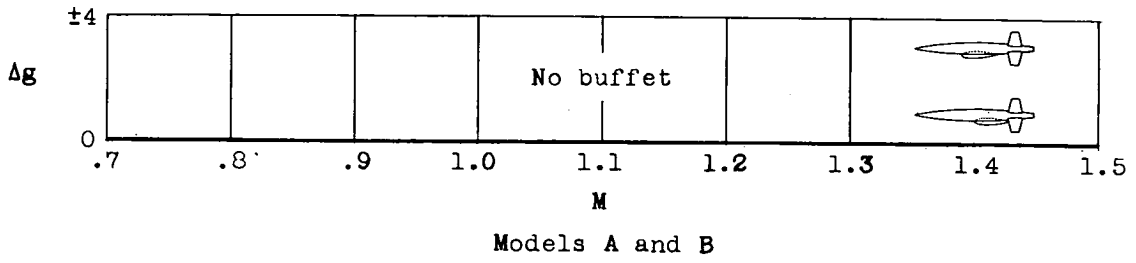
Model G



Model H

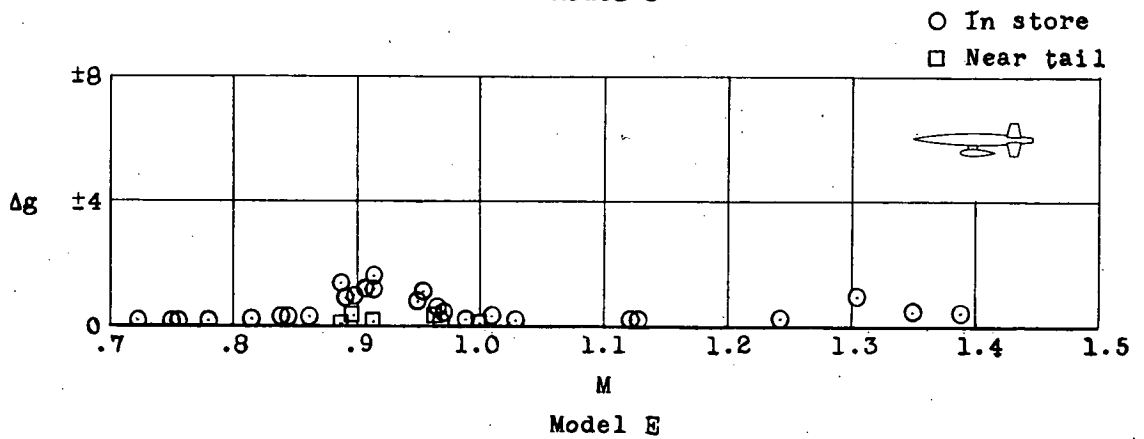
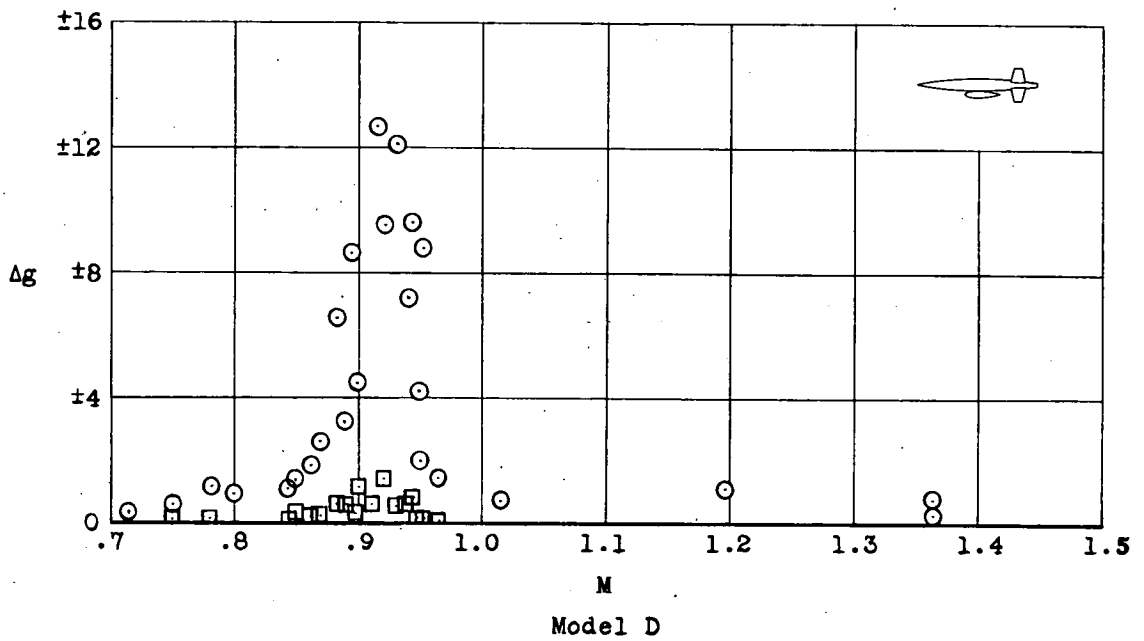
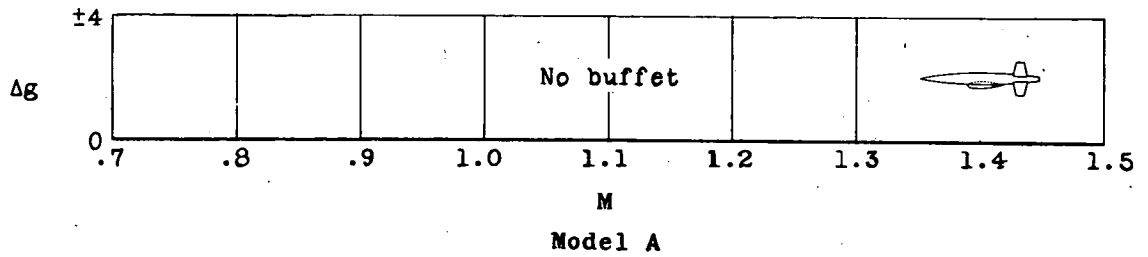
(b) At supersonic speeds for pylon-mounted models.

Figure 10.- Concluded.



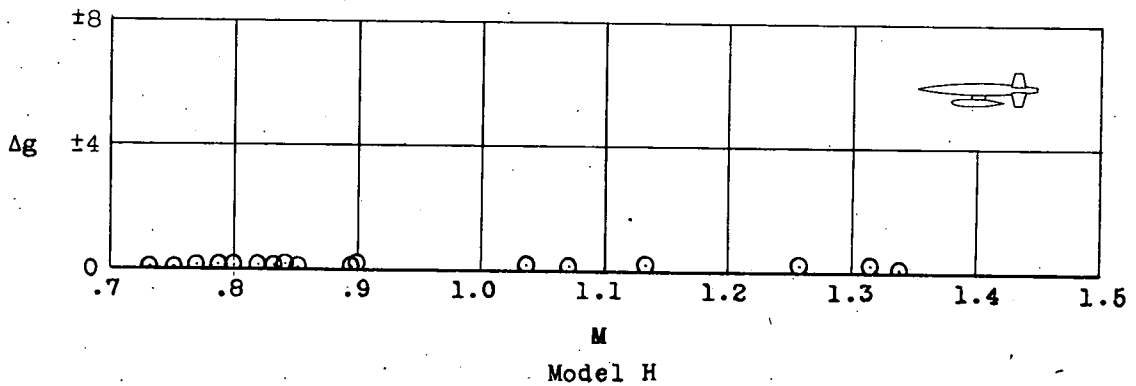
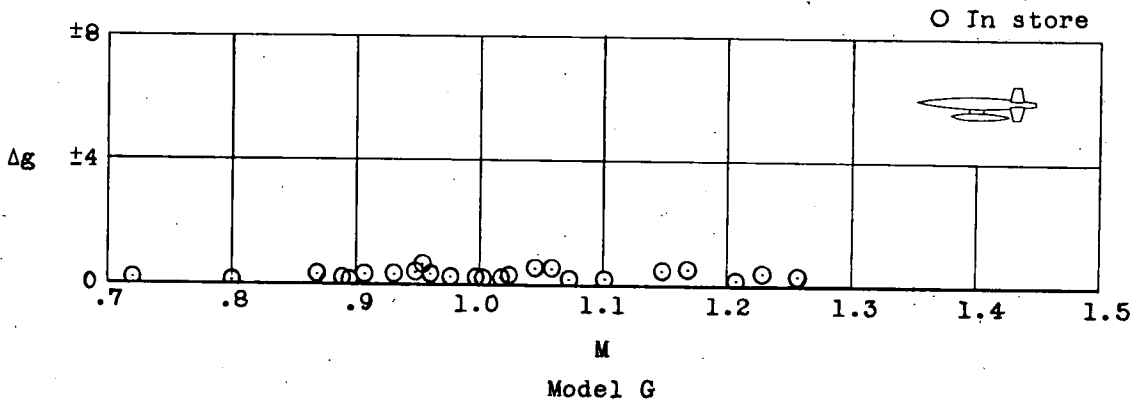
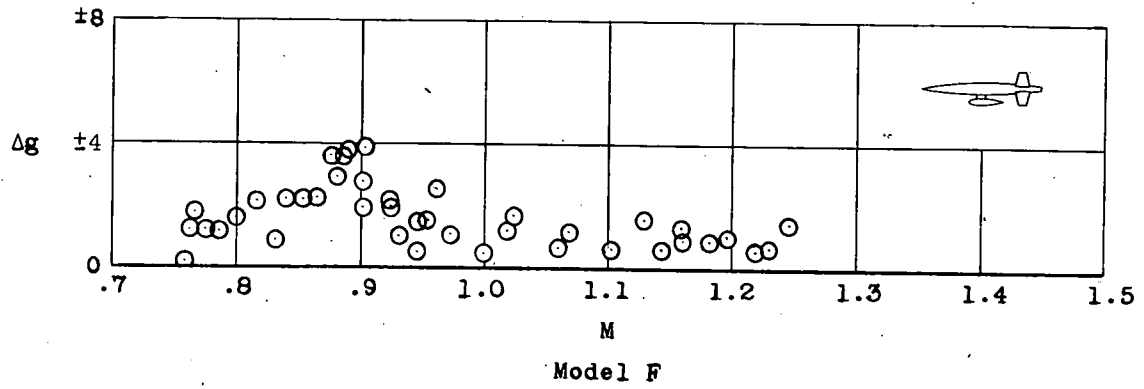
(a) Effect of semisubmerged store mounting.

Figure 11.- Variation of buffet intensity with Mach number.



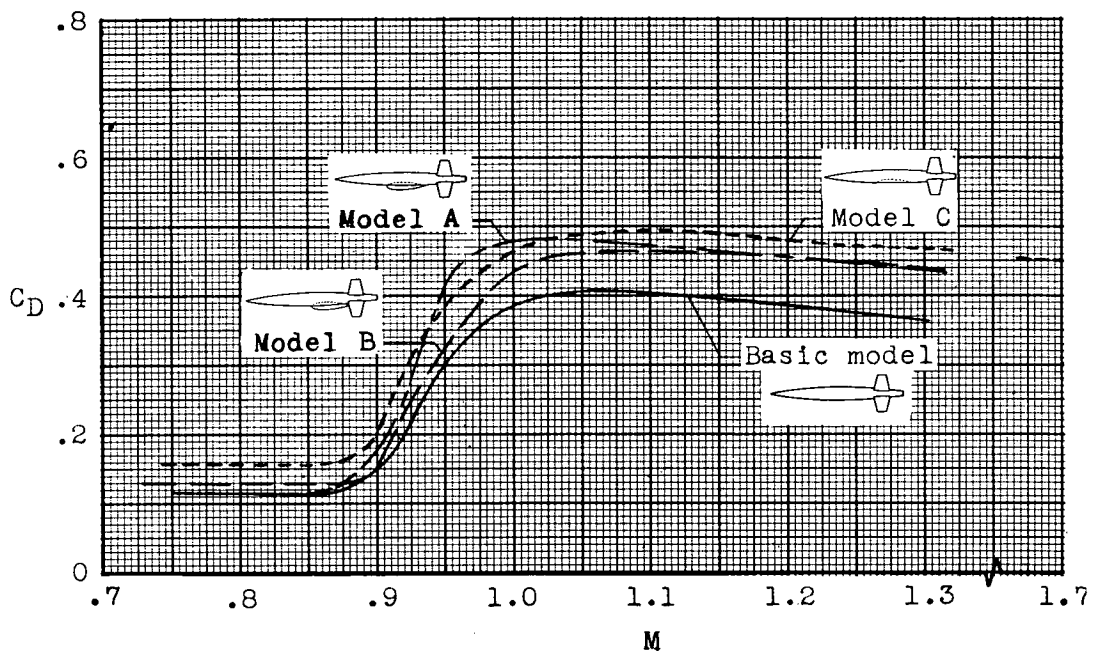
(b) Effect of vertical store location on the transverse buffet.

Figure 11.- Continued.

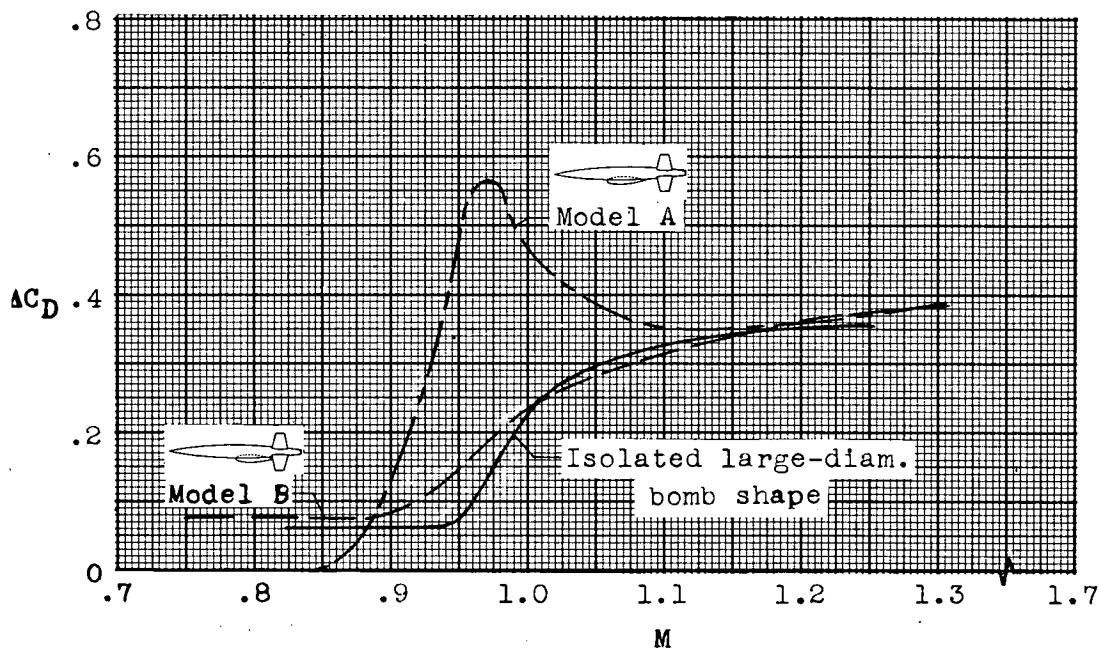


(c) Effect of store shape on the transverse buffet.

Figure 11.- Concluded.

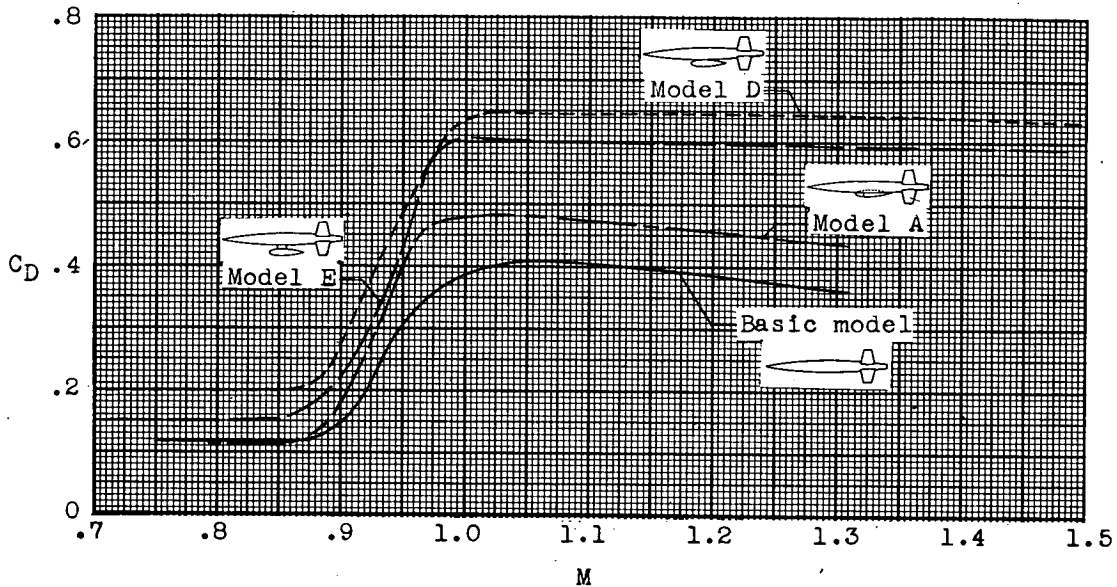


(a) Total drag based on body frontal area.

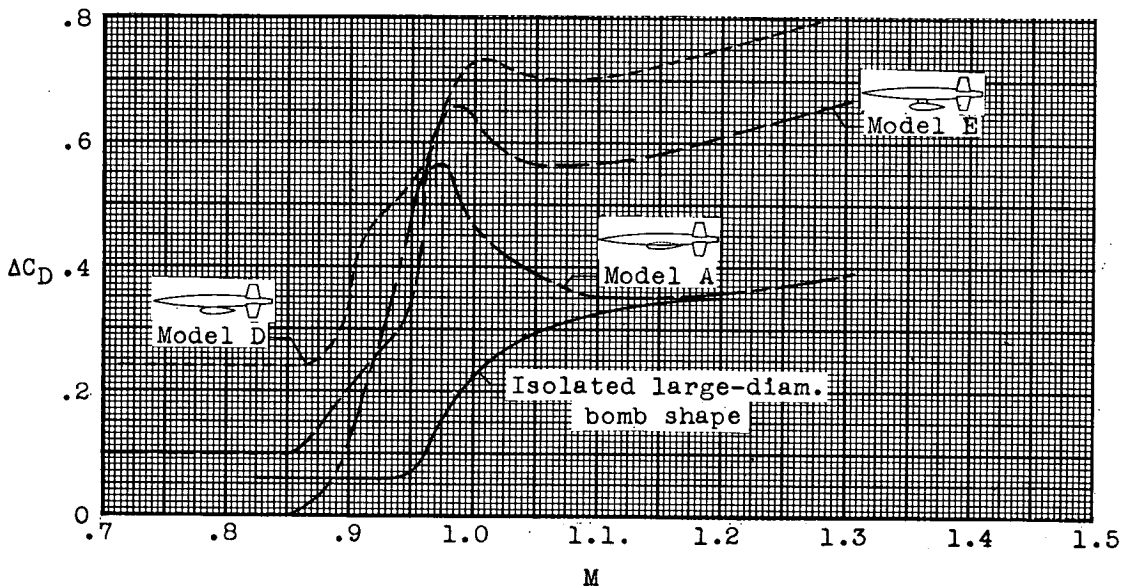


(b) Store plus interference drag based on store frontal area.

Figure 12.- Variation of drag with Mach number for semisubmerged store mounting.

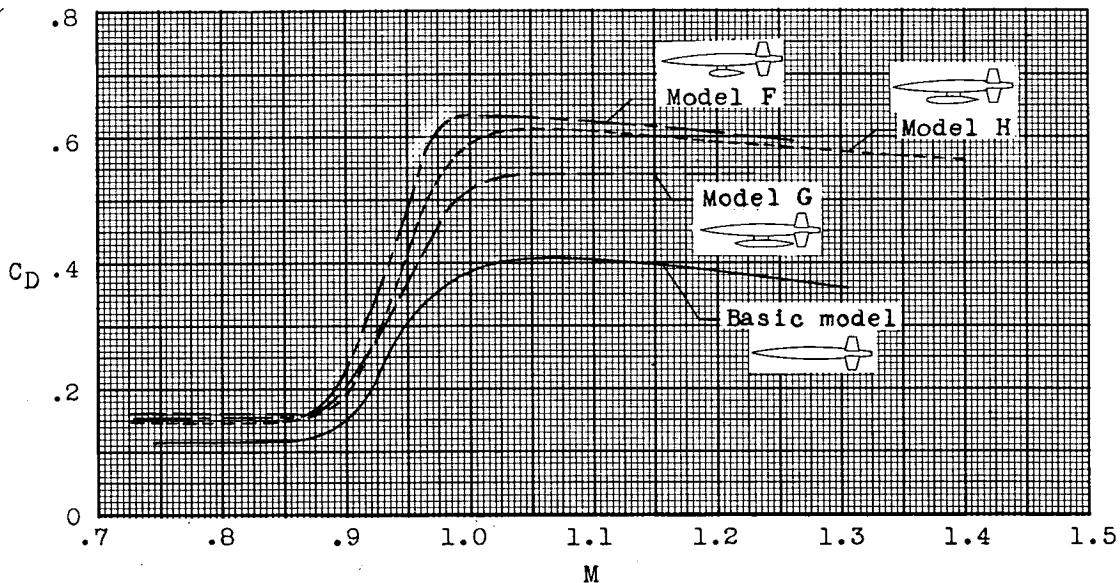


(a) Total drag based on body frontal area.

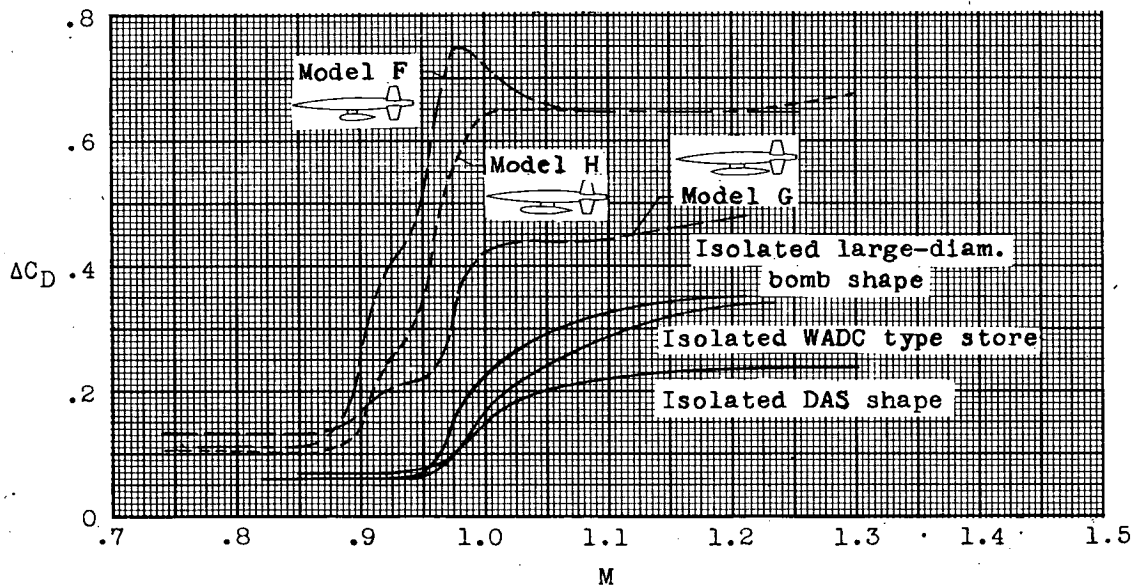


(b) Store plus interference drag based on store frontal area.

Figure 13.- Variation of drag with Mach number for various vertical store locations.



(a) Total drag based on body frontal area.



(b) Store plus interference drag based on store frontal area.

Figure 14.- Variation of drag with Mach number for different store shapes.

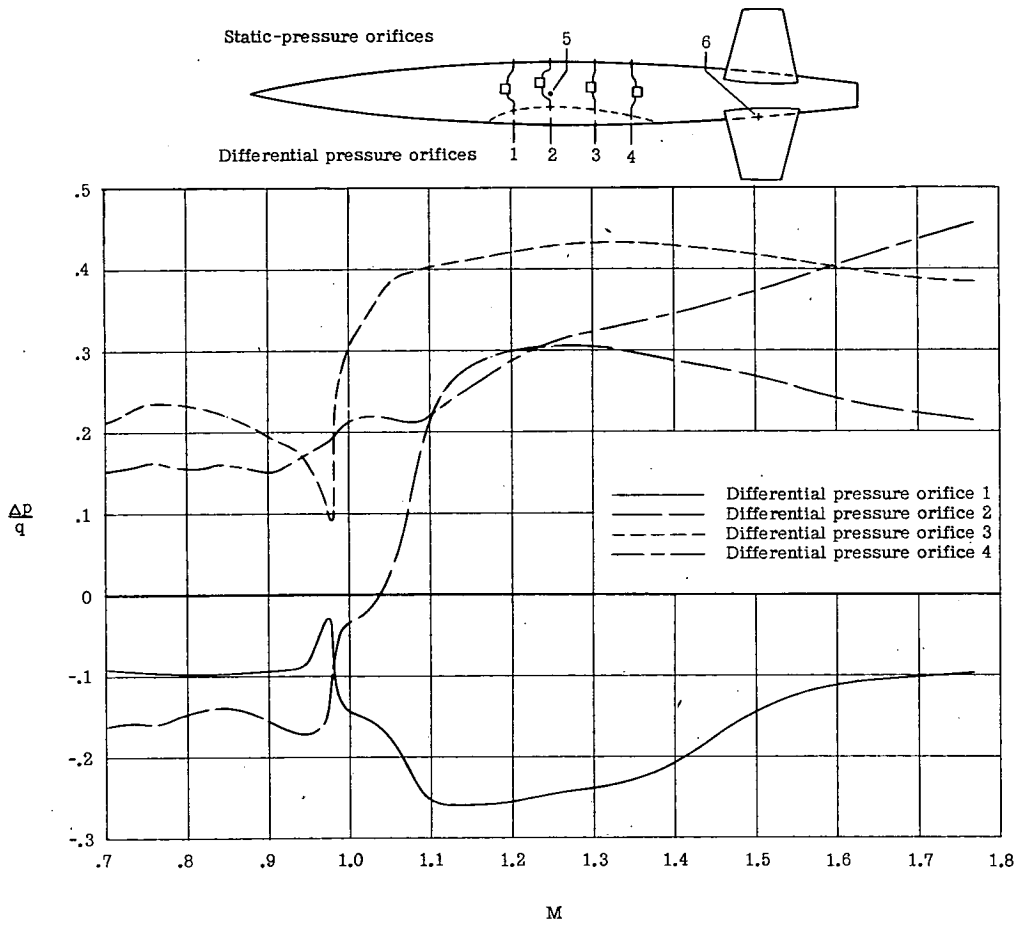


Figure 15.- Variation of cavity differential pressure with Mach number.

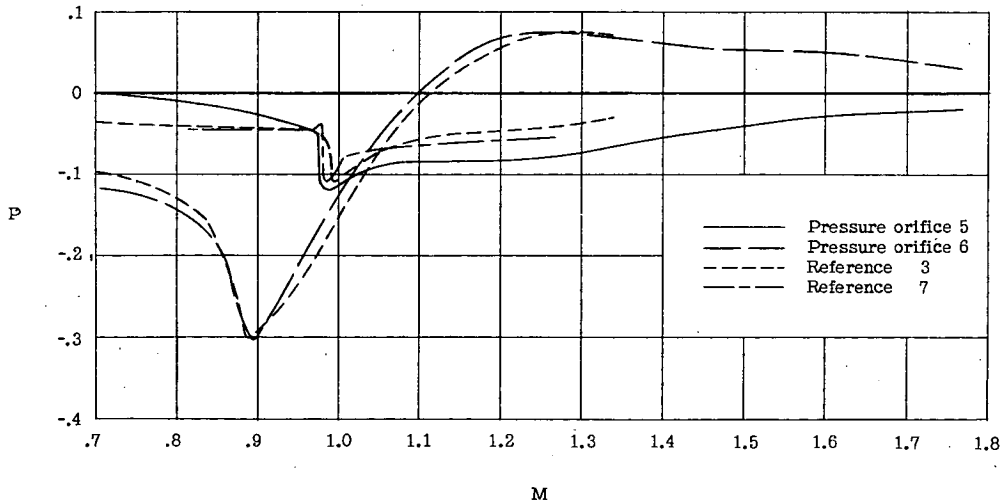


Figure 16.- Variation of pressure coefficient with Mach number.

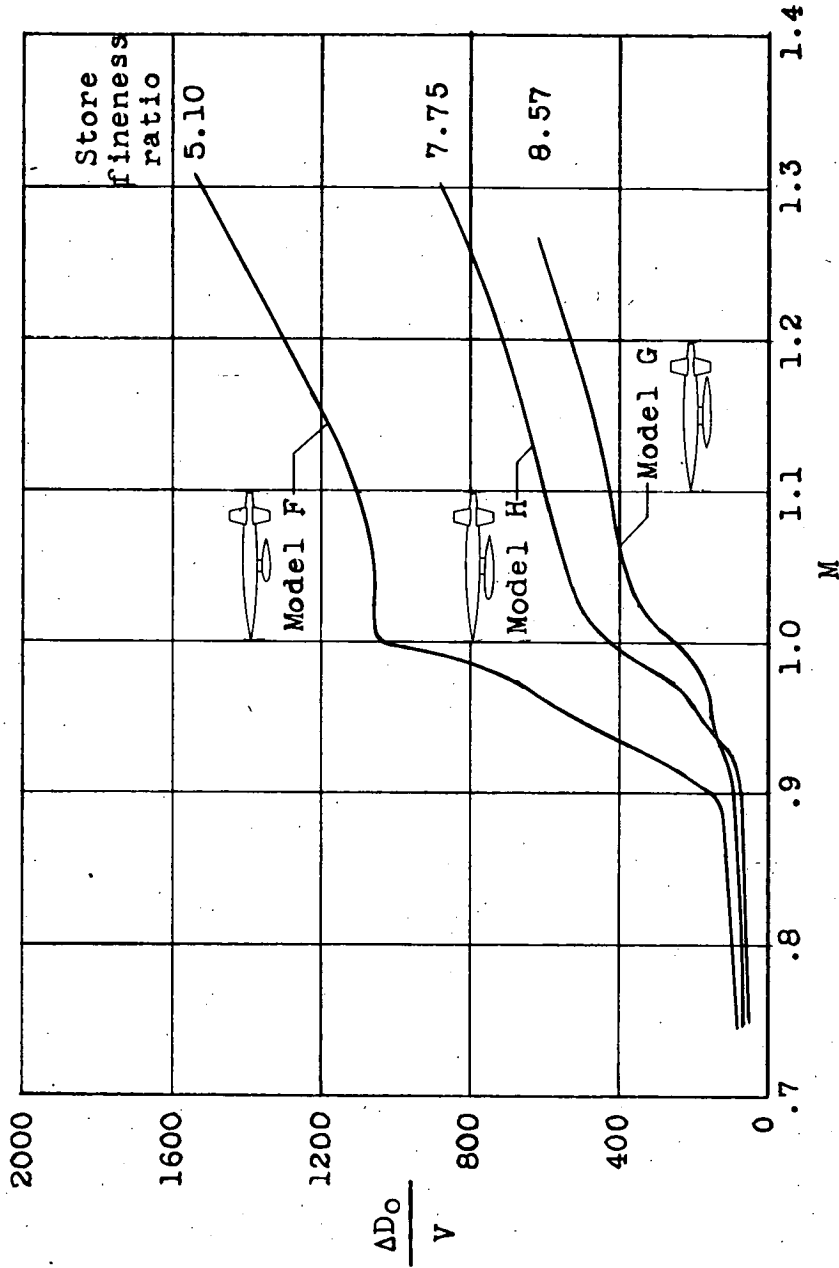
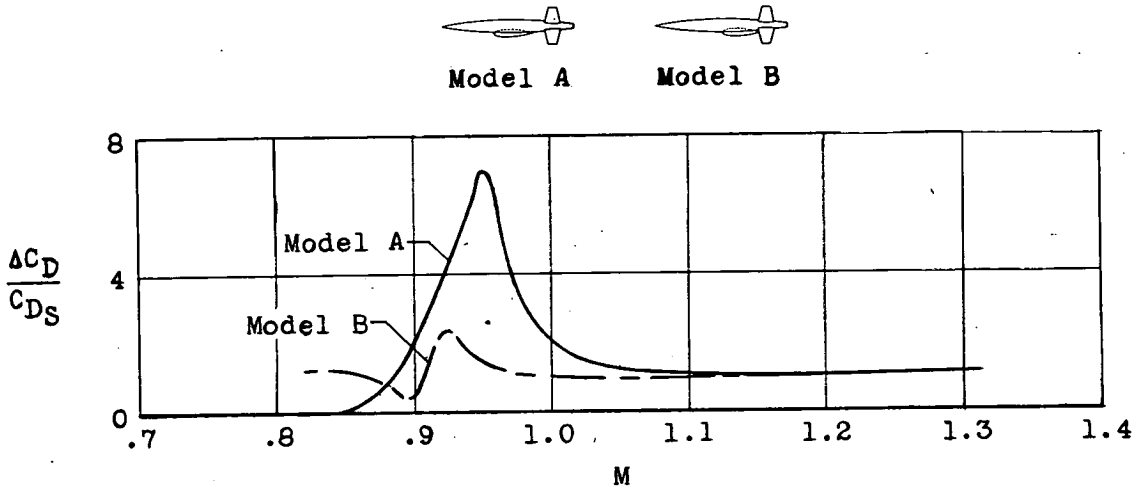
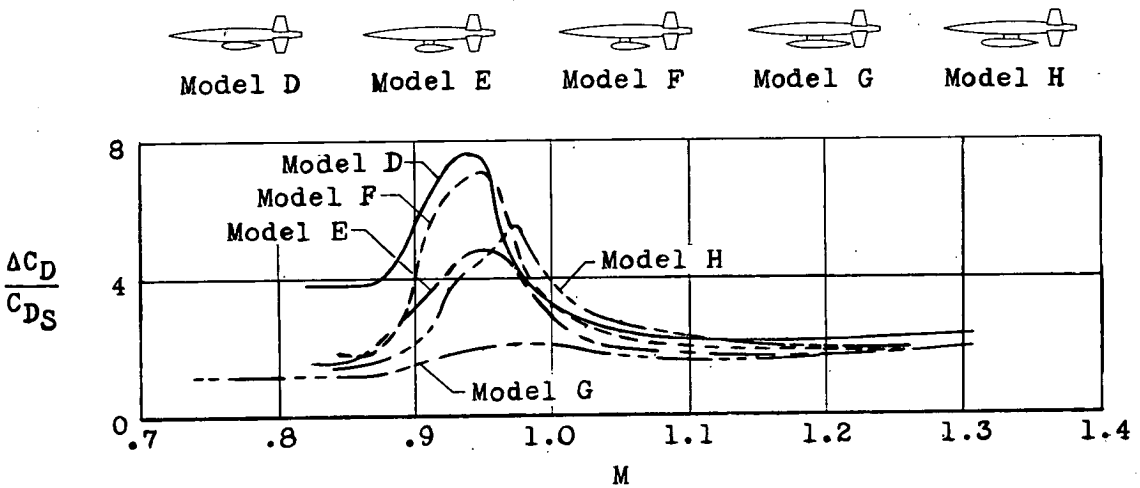


Figure 17.- Variation of installation drag per unit store volume with Mach number at sea-level standard conditions.



(a) Semisubmerged store mounting.



(b) External-store mountings.

Figure 18.- Variation of the ratio of installation drag to isolated-store drag with Mach number. Drag coefficients are based on store frontal area.